

SuperRL: Reinforcement Learning with Supervision to Boost Language Model Reasoning

Yihao Liu^{1*} Shuocheng Li^{1*} Lang Cao^{2*} Yuhang Xie^{1*}
 Mengyu Zhou^{3†} Haoyu Dong³ Xiaojun Ma³ Shi Han³ Dongmei Zhang³
¹Peking University ²University of Illinois Urbana-Champaign ³Microsoft

Abstract

Large language models (LLMs) are increasingly applied to complex reasoning tasks, where rich offline data—such as expert-annotated solutions or distilled traces—are often available. However, conventional reinforcement learning (RL) fails to exploit this data effectively, especially under sparse-reward environment. We propose SuperRL, a unified training framework to solve the problem. SuperRL employs an Adaptive Switch to detect reward sparsity and invokes a Hybrid Actor when rewards are sparse, blending policy gradients with offline supervision to stabilize learning. Experiments across diverse reasoning benchmarks demonstrate that SuperRL consistently outperforms standard RL, delivering improved sample efficiency, generalization, and robustness under sparse rewards.

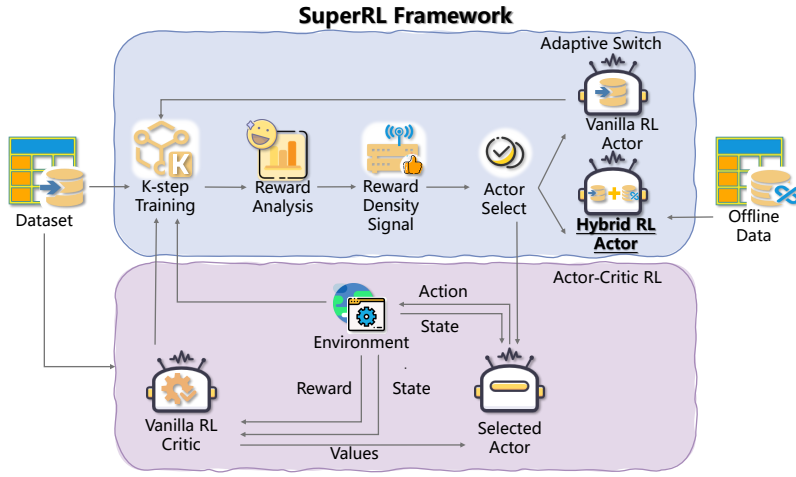


Figure 1: Overview of **SuperRL**. To adaptively optimize under varying reward conditions, SuperRL introduces an **Adaptive Switch** that conducts a brief rollout probe at the start of training to determine whether the environment provides dense or sparse rewards. In dense-reward settings, the model applies standard reinforcement learning (RL) updates to take full advantage of abundant feedback. When rewards are sparse, control is handed to a **Hybrid Actor** that augments the policy-gradient objective with a supervised fine-tuning (SFT) loss derived from high-quality offline trajectories. This hybrid update stabilizes learning and improves sample efficiency by compensating for insufficient or delayed reward signals. By dynamically switching objectives based on reward density, SuperRL effectively combines exploration with reliable offline supervision to support robust reasoning.

* Work done during internship at Microsoft.

† Corresponding author (mezho@microsoft.com).

1 Introduction

LLM reasoning has been studied extensively using lightweight prompting techniques—few-shot examples, chain-of-thought prompting, and self-consistency heuristics—but such static approaches can exhibit diminishing returns in more challenging inference scenarios. [1, 2, 3, 4, 5, 6] More recently, there has been growing interest in leveraging reinforcement learning for "test-time scaling" [7], empowering models to bolster their reasoning capabilities as they generate outputs. For example, Deepseek R1 demonstrates that applying Group Relative Policy Optimization (GRPO) to fine-tune inference trajectories can lead to more robust and flexible reasoning behaviors, all without modifying the underlying model architecture. [8, 9]

Despite recent progress, online reinforcement learning methods such as PPO and GRPO still face limitations in reasoning tasks. [8, 10] First, these inherently on-policy methods update exclusively from trajectories generated by the current policy and therefore struggle to leverage high-quality offline data—such as human-annotated or distilled reasoning traces—that encode valuable prior knowledge but lie outside the policy distribution. [11, 12] Second, in sparse-reward environments, online rollouts seldom produce enough successful trajectories to supply reliable learning signals, making it difficult to bootstrap coherent reasoning. [13, 14] Ultimately, because offline data provide numerous successful trajectories with clear guidance while online rollouts frequently fail and offer little feedback, reinforcement learning struggles to acquire robust reasoning capabilities in sparse-reward environments.

Supervised fine-tuning (SFT) directly leverages offline data with "correct thinking" to teach reliable reasoning paths but lacks any mechanism to learn from mistakes or negative cases, leading it to simply memorize positives [15, 16, 17]. In contrast, reinforcement learning (RL) can generalize by exploring and learning from failed trajectories [17]. While multi-stage SFT + RL—first offline fine-tuning then on-policy RL as in RLHF [18]—anchors models to sound reasoning and adapts them under sparse rewards, it suffers catastrophic forgetting of supervised knowledge during RL and considerable sample and compute inefficiency. [19, 20, 21] These shortcomings motivate tighter integration—e.g., interleaving or unifying SFT and RL objectives within each update—to preserve alignment, improve stability, and boost efficiency. However, multi-stage SFT+RL pipelines can impair generalization by overfitting to offline traces and narrow RL objectives. [19, 20, 21]

To enhance language model reasoning across both dense and sparse reward regimes, we propose **SuperRL**, a unified training framework built around two key components: the **Adaptive Switch** and the **Hybrid Actor**. The Adaptive Switch begins training with a brief rollout probe to determine whether the environment provides dense or sparse rewards. In dense-reward environment, SuperRL performs standard reinforcement learning updates to take advantage of abundant feedback. When rewards are sparse, control is handed over to the Hybrid Actor, which integrates reinforcement learning with supervised fine-tuning on high-quality offline reasoning traces—thus enabling the model to benefit from reliable "correct thinking" examples that standard on-policy methods are unable to effectively utilize. SuperRL is able to maintain robust, generalizable reasoning performance under sparse-reward conditions where traditional RL struggles to learn from valuable offline data.

As shown in Table 1, on sparse-reward datasets, SuperRL outperforms vanilla RL by large margins, +6.9% on LIMO, +15.0% on OpenR1, and +64.2% on HiTab. It also achieves notable generalization improvements on out-of-distribution datasets, demonstrating strong robustness under sparse-reward conditions. 4.3

Our main contributions are:

- We propose **SuperRL**, a unified training framework that adaptively switches between Vanilla and Hybrid RL actors based on the density of reward signals, enabling language models to reason effectively under both dense and sparse reward settings.
- We design a **Hybrid Actor** that interleaves policy-gradient updates with supervised fine-tuning on high-quality offline reasoning traces, striking a balance between exploration and reliable learning signals when rewards are sparse.
- We conduct comprehensive experiments across diverse datasets, model scales, and training regimes, demonstrating the robustness, effectiveness, and generalizability of the SuperRL framework in enhancing reasoning performance.

2 Related Work

2.1 Reasoning with LLMs

LLMs exhibit impressive knowledge but often struggle with complex reasoning tasks (e.g. multi-step math or logical problems) without specialized training. Recent research has shown that incorporating explicit reasoning steps can substantially improve performance. For example, training models to produce chain-of-thought solutions (step-by-step reasoning) enables better arithmetic and logic problem solving. [22] In fact, fine-tuning a pretrained LM on detailed quantitative reasoning demonstrations (as done in Minerva) led to state-of-the-art results on challenging math benchmarks. These findings underscore that vanilla next-token prediction alone is insufficient for high-level reasoning; additional fine-tuning or feedback signals are needed to guide LLMs in reasoning processes. This has driven interest in post-training LLMs specifically for reasoning capabilities, as seen with recent models like DeepSeek-R1, which explicitly target mathematical reasoning skills [22, 9]. Such models leverage verifiable rewards (e.g. checking a final answer’s correctness) to refine the reasoning ability of LLMs, pointing to the need for training paradigms beyond standard supervised learning. [9, 23]

2.2 Reinforcement Learning for LLMs

Reinforcement learning from human feedback [24]—as popularized by InstructGPT—uses on-policy methods like PPO to fine-tune language models against a learned reward signal, but doing so requires costly fresh sampling, a separate value network and careful KL-penalty tuning, and remains sample-inefficient when rewards are sparse. [10, 25, 22] GRPO simplifies PPO by ditching the critic and computing advantages via within-prompt reward normalization across multiple candidates, yet it still depends on large volumes of model-generated outputs and can wander from the pre-trained behavior in low-reward regimes. These limitations—computational overhead, sample inefficiency and instability under sparse feedback—have spurred interest in leaner or hybrid approaches that retain the simplicity of policy gradients while injecting external guidance to stabilize and steer training.[8, 22]

However, even with these leaner on-policy variants, sparse-reward reasoning still yields too few positive signals for stable gradient estimates, leading to stalled or collapsed training [13, 14].

2.3 Unifying SFT and RL: Towards Hybrid Optimization

Many methods leverage demonstrations to jump-start reasoning. SFT trains a pre-trained LLM on prompt–solution pairs (human-written or model-verified), teaching explicit reasoning patterns and yielding strong baseline performance.[26, 27] However, pure SFT merely imitates its training data: it cannot exceed the quality or coverage of provided solutions, and gaps in demonstration types or optimal answers limit its generalization.[17]

Recent research has demonstrated that combining supervised fine-tuning (SFT) with reinforcement learning (RL) effectively enhances the capabilities of large language models (LLMs). This approach leverages offline high-quality data to guide initial training and employs reinforcement learning to further align model outputs with desired behaviors. Notably, several recent works, including InstructGPT[27], DeepSeek-R1[9] and Qwen3[28], have adopted similar strategies to bolster the reasoning abilities of LLMs. [9, 28]

Unlike prior methods that apply supervised fine-tuning (SFT) and reinforcement learning (RL) in separate stages, SuperRL unifies them by injecting SFT signals directly into the RL loss function. This dynamic integration enables the model to simultaneously leverage the strengths of high-quality offline demonstrations and the exploratory benefits of online rollouts. By guiding policy updates with both supervised and reinforcement signals, SuperRL significantly improves reasoning capabilities and generalization performance. This unified optimization paradigm offers a principled framework for incorporating offline knowledge into reinforcement learning.

3 Methodology

We present SuperRL, a unified training framework comprising two key components—Adaptive Switch and Hybrid Actor—designed to adaptively train language models across both dense and sparse

reward environments. Unlike conventional SFT-RL pipelines, SuperRL dynamically monitors reward density and selects the appropriate training strategy: standard on-policy updates for dense rewards, or an integrated RL+SFT approach for sparse rewards. This preserves the sample efficiency of offline data while retaining the exploration benefits of reinforcement learning.

The Adaptive Switch conducts an initial rollout probe to assess reward density. If the average reward exceeds a predefined threshold, the model proceeds with vanilla actor–critic training. Otherwise, control is passed to the Hybrid Actor. This dynamic mechanism eliminates the need for manual scheduling and ensures automatic adaptation to varying reward structures, promoting stability and efficiency.

When activated, the Hybrid Actor blends policy-gradient updates with supervised fine-tuning on high-quality offline reasoning traces. By combining RL and SFT losses, the Hybrid Actor enhances learning in sparse-reward settings, improving convergence and robustness.

Together, these components form a single end-to-end training loop, unifying pre-training and fine-tuning. Under dense rewards, SuperRL operates as standard RL; under sparse rewards, it augments training with offline demonstrations. Full implementation and hyperparameter details are provided in this section.

3.1 Discussion of Adaptive Fusion of SFT and RL

We propose a adaptive fusion approach that integrates SFT and RL signals within each update step, dynamically weighted by uncertainty. Unlike traditional sequential paradigms where models undergo SFT followed by RL, our method continuously blends both objectives throughout training. This design captures the best of both worlds: the strong behavioral alignment of SFT and the exploratory capacity of RL. SFT provides rapid convergence toward expert-like behavior but often overfits and lacks robustness in unseen scenarios, especially under sparse rewards. [15, 16, 17] RL, on the other hand, promotes exploration and generalization but suffers from high variance and instability in low-signal environments. [17] Sequential SFT-RL pipelines often experience severe misalignment due to abrupt objective shifts, sometimes leading to catastrophic forgetting that RL alone cannot rectify. By contrast, our soft fusion strategy avoids such abrupt transitions. [19, 20, 21] Through uncertainty-based adaptive weighting, each update jointly incorporates both demonstration-driven and reward-driven signals, enabling more stable and efficient learning, particularly in sparse-reward settings.

The design yields two key benefits:

- **Stable early-stage learning:** In the presence of high uncertainty, the model leans more heavily on SFT signals, which encapsulate rich prior knowledge. This mitigates premature exploration and stabilizes initial training dynamics.
- **Resilient objective adaptation:** The framework continuously balances between SFT and reinforcement learning, dynamically prioritizing the more informative signal. This soft objective selection enables smooth adaptation to evolving task requirements, avoiding brittle transitions or model collapse.

We posit that this dynamic and continuous balance—rather than discrete handovers—forms the foundation of the model’s robustness and strong empirical performance in sparse-reward, reasoning-intensive tasks (see Appendix E for a comparative analysis of soft versus hard switching strategies).

3.2 Uncertainty-Weighted Hybrid Actor Design

To unify supervised and reinforcement learning objectives within a single optimization loop, we introduce an uncertainty-weighted hybrid actor. Concretely, we introduce two log-variance parameters, σ_{pg} and σ_{sft} , which respectively modulate the contributions of the policy-gradient loss L_{actor} and the SFT loss

$$L_{\text{sft}}(\theta) = \mathbb{E}_{(x,y) \sim D_{\text{sft}}} [\text{CrossEntropy}(\pi_\theta(y | x), y)].$$

Our hybrid objective is then written as

$$L_{\text{Hybrid}} = \exp(-2\sigma_{\text{pg}}) L_{\text{actor}} + \exp(-2\sigma_{\text{sft}}) L_{\text{sft}} + \sigma_{\text{pg}} + \sigma_{\text{sft}},$$

where L_{actor} can be instantiated by any policy-gradient method—e.g. PPO with its clipped surrogate

$$L_{\text{ppo}} = \mathbb{E}_t [\min(r_t A_t, \text{clip}(r_t, 1 - \epsilon, 1 + \epsilon) A_t)] - \beta_{\text{ent}} \mathbb{E}_t [\mathcal{H}(\pi_\theta)]$$

or GRPO, which further normalizes advantages within reasoning-template groups before clipping.

During training, we mix supervised fine-tuning (SFT) and reinforcement learning (RL) signals within each backward pass by interleaving high-quality demonstration data with on-policy rollouts. This design allows the model to learn from both expert behavior and exploration at the same time, ensuring that the two learning signals are tightly coupled throughout optimization.

To balance these signals, we use two learnable uncertainty parameters, σ_{pg} and σ_{sft} , which control how much each loss contributes. Noisy or unstable signals are automatically down-weighted through the exponential terms $\exp(-2\sigma)$, while the additive σ terms prevent the model from becoming over-confident. Because these weights are learned dynamically, the model adapts naturally to differences in signal quality without needing explicit switching rules.

This uncertainty-based fusion leads to more stable training, faster convergence, and stronger generalization—especially in sparse-reward, reasoning-heavy environments. By grounding updates in high-quality offline data while still allowing for on-policy exploration, our hybrid actor achieves better performance with a simpler and more unified training process.

3.3 Adaptive Switch Design

To dynamically select the most appropriate training strategy during the early stages of learning, we design a modular decision mechanism called the Adaptive Switch. This component allows SuperRL to automatically tailor its optimization behavior based on the reward characteristics of the environment, thereby avoiding rigid, one-size-fits-all solutions and improving generalization across diverse tasks.

Reward Density Assessment. Before formal training begins, SuperRL performs a lightweight rollout probe to assess the reward structure of the task. During this initial phase, the system executes a small number of pure RL training steps and monitors two key indicators: the average reward observed at each step and the number of times this average reward increases over the rollout window. Additionally, it calculates the average of the most recent few reward values to evaluate short-term learning progress. If both the increase count and the recent average reward fall below predefined thresholds, the task is classified as having sparse rewards; otherwise, it is treated as dense reward.

Based on this early analysis, the Adaptive Switch chooses the most suitable training actor. For dense-reward tasks, it selects a standard reinforcement learning actor, which benefits from the efficiency and alignment of pure policy-gradient updates. For sparse-reward tasks, it activates the proposed uncertainty-weighted hybrid actor, which incorporates supervised fine-tuning signals into every update. [4.2](#) [4.3](#)

We empirically determine effective threshold values for different batch size settings. When the batch size is larger than 32, we use 10 rollout steps, track the last 10 steps for recent average reward, and set the thresholds to 3 reward increases and a recent average reward of 0.1. For smaller batch sizes, we increase the number of rollout steps to 50, keep the recent average over 10 steps, and raise the thresholds to 20 increases and a recent average reward of 0.2. These values were selected based on extensive experiments across benchmarks such as GSM8K, MetaMath, LIMO, and so on. [4.5](#)

The modular nature of the Adaptive Switch makes it easy to interpret and customize. Practitioners can examine reward signals and actor decisions directly or override them using domain knowledge. This design not only streamlines system tuning but also enhances transparency and control.

Further extensions and discussions on the Adaptive Switch are provided in Appendix [A](#).

4 Experiments

4.1 Experimental Setup

We evaluate the SuperRL framework across a diverse set of reasoning-focused benchmarks, covering both in-domain and cross-domain generalization scenarios.

First, we investigate the learning and generalization capabilities of each approach across different datasets and evaluation sets. The results reveal that **pure RL excels in dense-reward environments**,

Table 1: Exact-match accuracy (%) across benchmarks using **Qwen2.5-1.5B** with GRPO. The RL baseline (gray) is compared to other methods, with deviations highlighted in green (gains) and red (drops); color intensity reflects magnitude. Rows are grouped by training dataset. Hybrid refers to the Hybrid Actor.

Training	Method	GSM8K	MetaMath	PRM12K	LIMO	OpenR1	HiTab
GSM8K	RL	77.1	83.9	46.7	6.7	10.6	1.2
	SFT	59.7	64.5	26.7	1.2	7.4	0.0
	SFT+RL	74.7	77.3	35.1	6.7	9.8	0.0
	Hybrid	77.0	79.9	14.0	2.6	14.1	1.7
MetaMath	RL	74.0	81.7	50.8	5.0	12.5	6.0
	SFT	70.1	76.5	33.9	2.4	7.9	0.0
	SFT+RL	75.2	78.7	38.7	5.5	9.7	0.2
	Hybrid	79.5	82.6	33.0	1.8	15.4	1.1
PRM12K	RL	74.1	78.3	50.5	9.8	14.2	2.8
	SFT	7.1	41.7	29.2	1.2	6.4	0.0
	SFT+RL	69.2	74.3	47.7	8.5	13.2	0.0
	Hybrid	72.0	74.8	50.3	11.0	15.7	3.3
OpenR1	RL	3.0	3.3	10.0	9.1	0.0	0.0
	SFT	43.4	61.2	36.4	4.9	10.4	1.2
	SFT+RL	69.7	72.9	46.5	9.1	15.7	2.1
	Hybrid	70.0	72.7	46.0	9.8	15.0	10.4
LIMO	RL	0.0	0.0	0.0	0.0	0.4	0.0
	SFT	16.3	17.3	10.8	1.2	1.8	0.7
	SFT+RL	28.7	48.7	19.3	3.0	3.2	0.0
	Hybrid	70.0	72.7	47.2	6.9	7.6	0.1
HiTab	RL	16.9	37.2	27.7	0.1	6.9	0.0
	SFT	33.2	54.4	46.5	4.9	12.7	5.5
	SFT+RL	35.7	36.6	30.1	9.1	14.0	60.7
	Hybrid	44.1	41.2	34.7	5.5	8.8	64.2

while **Hybrid Actor achieves the best performance under sparse-reward environments**, where both RL and sequential SFT+RL struggle. These findings delineate the effective operating regimes of each method and highlight the necessity of the Adaptive Switch.

Second, we demonstrate the generalizability of the Hybrid Actor design across multiple reinforcement learning algorithms (e.g., PPO and GRPO) and model scales (ranging from 1B to 8B). In most settings under sparse-reward conditions, hybrid yields better convergence, improved generalization, and more stable updates.

Third, we analyze the the Adaptive Switch module, showing how it accurately identifies reward density through early training probes and dynamically selects the appropriate training actor. Our results provide clear empirical support for its decision logic, ensuring optimal strategy selection without manual intervention.

Complete experimental settings, switch thresholds, and implementation details are provided in Appendix C.7 and Appendix C.8.

4.2 RL Dominates in Dense-Reward Reasoning Tasks

Dense reward environments are characterized by frequent and informative feedback at each step of the generation process. This setting provides clear optimization signals, allowing models to efficiently explore the solution space without relying heavily on supervised demonstrations. Arithmetic and symbolic reasoning tasks with low output variability often fall into this category, making them well-suited for reinforcement learning. In Table 1, datasets such as GSM8K, METAMATHQA, and PRM12K exemplify dense reward settings. Across these benchmarks, RL demonstrates strong performance, highlighting its ability to exploit dense supervision for effective learning and generalization.

Table 2: KL-loss range and variance comparison: RL vs Hybrid Actor

Dataset	KL Range (RL)	KL Range (Hybrid)	Max Δ	KL Var (RL)	KL Var (Hybrid)	Var Δ
MetaMath	[2.63e ⁻⁴ , 0.6055]	[8.59e ⁻⁴ , 0.2732]	-54.9%	0.009388	0.002664	-71.6%
GSM8K	[7.93e ⁻⁴ , 0.5306]	[7.17e ⁻⁴ , 0.2770]	-47.8%	0.007579	0.002475	-67.3%
PRM12K	[5.68e ⁻⁴ , 0.2616]	[7.96e ⁻⁴ , 0.0900]	-66.0%	0.002159	0.000379	-82.4%
LIMO	[3.60e ⁻⁴ , 0.7732]	[3.59e ⁻⁴ , 0.2391]	-69.1%	0.02489	0.001494	-94.0%
OpenR1	[3.01e ⁻⁴ , 1.9110]	[6.78e ⁻⁴ , 0.0952]	-95.0%	0.01637	0.000239	-98.5%
HiTab	[7.58e ⁻⁴ , 1.9600]	[6.59e ⁻⁴ , 1.0387]	-47.0%	0.006257	0.01079	+72.4%

RL demonstrates strong performance under dense reward settings, achieving the highest accuracy on in-domain tasks and exhibiting superior generalization compared to all other methods. Concretely, when trained on GSM8K, RL achieves an exact-match accuracy of **77.1%**, outperforming other methods. A similar pattern holds on METAMATHQA, where RL reaches **81.7%**, surpassing SFT (**76.5%**) and SFT+RL (**78.7%**). These results highlight RL’s ability to effectively leverage dense and well-aligned reward signals. Moreover, RL exhibits strong cross-task generalization. When trained on GSM8K and evaluated on PRM12K, RL attains an accuracy of **46.7%**, significantly outperforming SFT (**26.7%**), SFT+RL (**35.1%**), and the Hybrid method (**14.0%**). The pattern can be extended to all the three datasets mentioned above. This suggests that RL-learned policies capture transferable reasoning patterns that extend beyond the source task.

4.3 Hybrid Actor Thrives in Sparse-Reward Reasoning Tasks

Sparse reward settings are characterized by infrequent or weak reward signals, often posing significant challenges to exploration and optimization. Datasets such as LIMO, OPENR1, and HiTAB exemplify this regime.

In these environments, hybrid consistently outperforms other methods. For instance, on HiTAB, where RL fails to learn (0.0%), the hybrid model achieves **64.2%** accuracy—exceeding SFT+RL (**60.7%**) and SFT (**5.5%**). Similar gains are observed on OPENR1 and LIMO, where the hybrid method retains strong performance despite limited supervision. Notably, this robustness extends beyond symbolic reasoning tasks to semi-structured domains like TableQA dataset HiTAB, highlighting the Hybrid Actor’s ability to generalize across diverse reasoning tasks.

Beyond accuracy, Hybrid Actor enhances both learning stability and generalization, especially when compared to the SFT+RL method. Unlike SFT+RL, which suffers from abrupt shifts between supervised and reinforcement phases, Hybrid Actor maintains a continuous inductive prior, leading to smoother updates and more consistent optimization. As shown in Table 2, Hybrid Actor significantly reduces KL-loss variance across challenging tasks, achieving reductions of **71.6%** on METAMATH, **67.3%** on GSM8K, and up to **98.5%** on OPENR1. These reductions indicate fewer erratic updates and greater training stability. On HiTAB, the KL variance under Hybrid Actor is higher (**+72.4%**)—not due to instability, but because reward signals in this dataset remain consistently zero,

These stability benefits also lead to stronger generalization across diverse reasoning tasks. For example, when trained on LIMO—a sparse-reward dataset where vanilla RL completely fails (**0.0%** across all benchmarks)—Hybrid Actor achieves remarkable accuracy across the board: **70.0%** on GSM8K, **72.7%** on METAMATH, **47.2%** on PRM12K, and **6.9%** on LIMO itself. These results substantially surpass both SFT+RL and SFT, which often collapse under sparse reward: e.g., SFT+RL yields only **28.7%** on GSM8K and **48.7%** on METAMATH, while SFT achieves **16.3%** and **17.3%** respectively. Similarly, when trained on HiTAB, Hybrid attains the highest in-domain accuracy of **64.2%**, outperforming both SFT+RL (**60.7%**) and SFT (**5.5%**) by large margins. Even on out-of-domain tasks like METAMATH and PRM12K, Hybrid maintains competitive performance, demonstrating robust transferability. These results underscore the advantages of Hybrid Actor in leveraging supervised demonstrations while maintaining the exploratory flexibility of reinforcement learning. By integrating both signals throughout training, it avoids brittle mode transitions and achieves consistently strong performance across domains—particularly in sparse-reward environments where traditional pipelines often fail to generalize.

Table 3: Exact-match accuracy (%) on GSM8K, PRM12K, and LIMO when trained on LIMO using **Qwen2.5-1.5B** under PPO and GRPO. Vanilla baselines are shown in gray; gains/losses are highlighted in green/red. Hybrid refers to the Hybrid Actor.

Optimizer	Method	GSM8K	PRM12K	LIMO
PPO	PPO	52.5	29.9	4.9
	SFT	59.7	26.7	1.2
	SFT+PPO	70.3	44.4	8.5
	PPO Hybrid	67.7	48.6	11.6
GRPO	GRPO	0.0	0.0	0.0
	SFT	59.7	26.7	1.2
	SFT+GRPO	28.7	19.3	3.0
	GRPO Hybrid	70.0	47.2	6.9

4.4 Generalization Study

The Hybrid Actor enables stable, transferable learning across different RL algorithms To assess generalization across RL algorithms in sparse-reward settings, we evaluate our Hybrid Actor under both PPO and GRPO using the same model architecture (Qwen2.5-1.5B) and training data (LIMO). As shown in Table 3, Hybrid consistently outperforms both vanilla RL and SFT+RL baselines. Under PPO, Hybrid Actor achieves +18.7% and +6.7% improvements over vanilla PPO on PRM12K and LIMO, respectively. Compared to the stronger SFT+PPO pipeline, Hybrid still yields notable gains: +4.2% on PRM12K and +3.1% on LIMO. Under GRPO, Hybrid delivers even larger margins: +70.0% on GSM8K, +47.2% on PRM12K, and +6.9% on LIMO compared to the vanilla GRPO baseline, which fails to learn effectively. Even when compared to SFT+GRPO, Hybrid achieves consistent gains of +41.3%, +27.9%, and +3.9% on GSM8K, PRM12K, and LIMO, respectively.

Table 4: Exact-match accuracy (%) on GSM8K, PRM12K, HiTab, and LIMO when trained on HiTAB using PPO and Hybrid across model scales. PPO serves as baseline (gray); improvements/degradations from Hybrid are shown in green/red. Hybrid refers to the Hybrid Actor.

Model	Method	GSM8K	PRM12K	HiTab	LIMO
Qwen2.5 1.5B	PPO	46.9	30.4	0.1	5.5
	Hybrid	43.1	30.6	0.5	5.5
Qwen2.5 3B	PPO	68.5	49.1	16.3	12.8
	Hybrid	72.1	55.3	53.7	15.2
Qwen2.5 7B	PPO	86.6	59.6	65.5	21.3
	Hybrid	83.8	63.7	76.4	28.1
LLaMA3.2 1B	PPO	41.6	31.9	0.8	6.7
	Hybrid	40.5	25.1	0.1	7.3
LLaMA3.2 3B	PPO	74.2	53.2	48.4	20.1
	Hybrid	74.2	53.8	61.9	23.2
LLaMA3.1 8B	PPO	82.3	55.3	68.8	20.1
	Hybrid	82.0	54.6	77.7	20.1

The Hybrid Actor generalizes across model scales and architectures. Table 4 presents exact-match accuracy across four datasets when models are trained on HiTAB. For smaller models like Qwen2.5-1.5B and LLaMA3.2-1B, Hybrid yields mixed results, with minor regressions on GSM8K and PRM12K. However, starting from the 3B scale, Hybrid begins to outperform PPO. For example, on Qwen2.5-3B, Hybrid achieves +6.2% on PRM12K and a substantial +37.4% on HiTab. The gains persist on Qwen2.5-7B, with Hybrid reaching +10.9% improvement on HiTab and +6.8% on LIMO. Similarly, for LLaMA3.2-3B, Hybrid improves HiTab accuracy from 48.4% to 61.9%. These results indicate that the advantages of Hybrid training persist across both model scales and architectures (e.g., Qwen and LLaMA), demonstrating its robustness and effectiveness in sparse-reward environments.

4.5 Empirical Study on K-step Training Parameters for Adaptive Switch

In this section, we discuss the parameter settings of Adaptive Switch in SuperRL. In the Appendix C.8, we study the impact of different initialization values of σ_{pg} and σ_{sft} for Hybrid Actor. Here, we focus on the appropriate values for the parameters related to the K-step training.

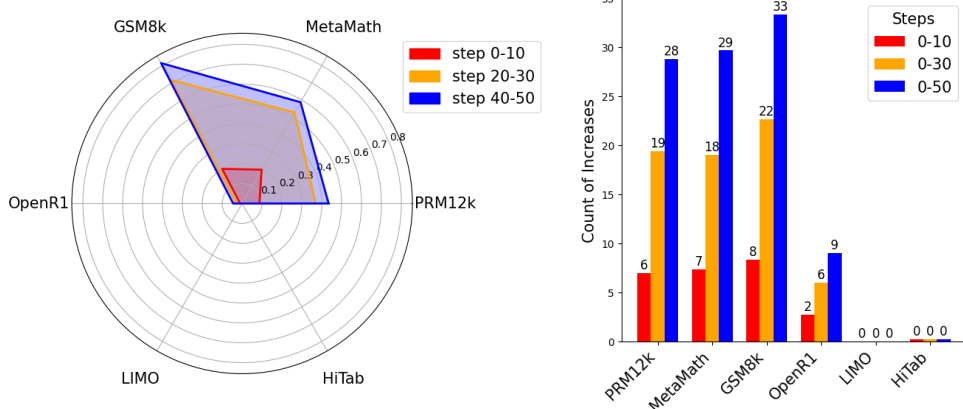


Figure 2: Average Reward Values on Different Benchmarks (0-10, 20-30, 40-50 Steps)

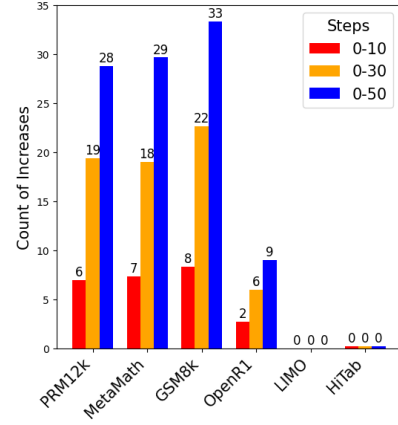


Figure 3: Count of Reward Increases on Different Benchmarks (0-10, 0-30, 0-50 Steps)

We propose a reward-based switching strategy to assess the effectiveness of RL during early training for Adaptive Switch. If early rewards are sparse—characterized by stagnant or low rewards—the system transitions to a hybrid training mode, improving learning stability in sparse-reward settings.

After k steps of RL training, we compute the average reward (avg_reward) at each step and derive two metrics: the number of reward increases across steps (increase_num) and the average reward over the last m steps (recent_avg_reward). A mode switch is triggered if both $\text{increase_num} < \text{increase_threshold}$ and $\text{recent_avg_reward} < \text{avg_threshold}$.

Table 7 in the Appendix illustrates early reward dynamics during the first 10 steps of GRPO training with Qwen2.5-1.5B on GSM8K and HiTAB. On GSM8K, the initially low average reward (avg_reward) increases rapidly, reaching 0.4894 by step 10. This indicates that standard RL training progresses effectively, and no switching is required. In contrast, on HiTAB, both the number of reward increases (increase_num) and the recent average reward (recent_avg_reward) remain near zero, signaling training stagnation and prompting a mode switch.

Figures 2 and 3 provide further insight by plotting the average reward and cumulative count of reward increases across early training steps for Qwen2.5-1.5B on multiple benchmarks. As shown, easier datasets such as GSM8K and METAMATH exhibit steady increases in both metrics, while harder datasets like LIMO and HiTAB show little to no improvement. Based on these observations, we empirically set the switch parameters as follows: for batch sizes larger than 32, we use $k = 10$, $m = 10$, $\text{increase_threshold} = 3$, and $\text{recent_avg_reward} = 0.1$; otherwise, we set $k = 50$, $m = 10$, $\text{increase_threshold} = 20$, and $\text{recent_avg_reward} = 0.2$. Full details of the experimental setup are provided in Appendix C.8.

5 Conclusion

We present SuperRL, a unified training framework that adaptively combines supervised and reinforcement signals to improve reasoning under both dense and sparse rewards. Experiments show that SuperRL achieves superior performance, stability, and generalization across diverse reasoning benchmarks. Limitations and future work are discussed in Appendix A.

References

- [1] Jason Wei, Xuezhi Wang, Dale Schuurmans, Maarten Bosma, Fei Xia, Ed Chi, Quoc V Le, Denny Zhou, et al. Chain-of-thought prompting elicits reasoning in large language models. *Advances in neural information processing systems*, 35:24824–24837, 2022.
- [2] Xuezhi Wang, Jason Wei, Dale Schuurmans, Quoc Le, Ed Chi, Sharan Narang, Aakanksha Chowdhery, and Denny Zhou. Self-consistency improves chain of thought reasoning in language models. *arXiv preprint arXiv:2203.11171*, 2022.
- [3] Tom Brown, Benjamin Mann, Nick Ryder, Melanie Subbiah, Jared D Kaplan, Prafulla Dhariwal, Arvind Neelakantan, Pranav Shyam, Girish Sastry, Amanda Askell, et al. Language models are few-shot learners. *Advances in neural information processing systems*, 33:1877–1901, 2020.
- [4] Boshi Wang, Sewon Min, Xiang Deng, Jiaming Shen, You Wu, Luke Zettlemoyer, and Huan Sun. Towards understanding chain-of-thought prompting: An empirical study of what matters. *arXiv preprint arXiv:2212.10001*, 2022.
- [5] Zhiusheng Zhang, Aston Zhang, Mu Li, and Alex Smola. Automatic chain of thought prompting in large language models. *arXiv preprint arXiv:2210.03493*, 2022.
- [6] Lang Cao. Graphreason: Enhancing reasoning capabilities of large language models through a graph-based verification approach. *arXiv preprint arXiv:2308.09267*, 2023.
- [7] Qiyuan Zhang, Fuyuan Lyu, Zexu Sun, Lei Wang, Weixu Zhang, Wenyue Hua, Haolun Wu, Zhihan Guo, Yufei Wang, Niklas Muennighoff, Irwin King, Xue Liu, and Chen Ma. A survey on test-time scaling in large language models: What, how, where, and how well?, 2025.
- [8] Zhihong Shao, Peiyi Wang, Qihao Zhu, Runxin Xu, Junxiao Song, Xiao Bi, Haowei Zhang, Mingchuan Zhang, YK Li, Y Wu, et al. Deepseekmath: Pushing the limits of mathematical reasoning in open language models. *arXiv preprint arXiv:2402.03300*, 2024.
- [9] DeepSeek-AI, Daya Guo, Dejian Yang, Haowei Zhang, Junxiao Song, Ruoyu Zhang, Runxin Xu, Qihao Zhu, Shirong Ma, Peiyi Wang, Xiao Bi, Xiaokang Zhang, Xingkai Yu, Yu Wu, Z. F. Wu, Zhibin Gou, Zhihong Shao, Zhuoshu Li, Ziyi Gao, Aixin Liu, Bing Xue, Bingxuan Wang, Bochao Wu, Bei Feng, Chengda Lu, Chenggang Zhao, Chengqi Deng, Chenyu Zhang, Chong Ruan, Damai Dai, Deli Chen, Dongjie Ji, Erhang Li, Fangyun Lin, Fucong Dai, Fuli Luo, Guangbo Hao, Guanting Chen, Guowei Li, H. Zhang, Han Bao, Hanwei Xu, Haocheng Wang, Honghui Ding, Huajian Xin, Huazuo Gao, Hui Qu, Hui Li, Jianzhong Guo, Jiashi Li, Jiawei Wang, Jingchang Chen, Jingyang Yuan, Junjie Qiu, Junlong Li, J. L. Cai, Jiaqi Ni, Jian Liang, Jin Chen, Kai Dong, Kai Hu, Kaige Gao, Kang Guan, Kexin Huang, Kuai Yu, Lean Wang, Lecong Zhang, Liang Zhao, Litong Wang, Liyue Zhang, Lei Xu, Leyi Xia, Mingchuan Zhang, Minghua Zhang, Minghui Tang, Meng Li, Miaojun Wang, Mingming Li, Ning Tian, Panpan Huang, Peng Zhang, Qiancheng Wang, Qinyu Chen, Qiushi Du, Ruiqi Ge, Ruisong Zhang, Ruizhe Pan, Runji Wang, R. J. Chen, R. L. Jin, Ruyi Chen, Shanghao Lu, Shangyan Zhou, Shanhuan Chen, Shengfeng Ye, Shiyu Wang, Shuiping Yu, Shunfeng Zhou, Shuting Pan, S. S. Li, Shuang Zhou, Shaoqing Wu, Shengfeng Ye, Tao Yun, Tian Pei, Tianyu Sun, T. Wang, Wangding Zeng, Wanjia Zhao, Wen Liu, Wenfeng Liang, Wenjun Gao, Wenqin Yu, Wentao Zhang, W. L. Xiao, Wei An, Xiaodong Liu, Xiaohan Wang, Xiaokang Chen, Xiaotao Nie, Xin Cheng, Xin Liu, Xin Xie, Xingchao Liu, Xinyu Yang, Xinyuan Li, Xuecheng Su, Xuheng Lin, X. Q. Li, Xiangyue Jin, Xiaojin Shen, Xiaosha Chen, Xiaowen Sun, Xiaoxiang Wang, Xinnan Song, Xinyi Zhou, Xianzu Wang, Xinxia Shan, Y. K. Li, Y. Q. Wang, Y. X. Wei, Yang Zhang, Yanhong Xu, Yao Li, Yao Zhao, Yaofeng Sun, Yaohui Wang, Yi Yu, Yichao Zhang, Yifan Shi, Yiliang Xiong, Ying He, Yishi Piao, Yisong Wang, Yixuan Tan, Yiyang Ma, Yiyuan Liu, Yongqiang Guo, Yuan Ou, Yuduan Wang, Yue Gong, Yuheng Zou, Yujia He, Yunfan Xiong, Yuxiang Luo, Yuxiang You, Yuxuan Liu, Yuyang Zhou, Y. X. Zhu, Yanhong Xu, Yanping Huang, Yaohui Li, Yi Zheng, Yuchen Zhu, Yunxian Ma, Ying Tang, Yukun Zha, Yuting Yan, Z. Z. Ren, Zehui Ren, Zhangli Sha, Zhe Fu, Zhean Xu, Zhenda Xie, Zhengyan Zhang, Zhewen Hao, Zhicheng Ma, Zhigang Yan, Zhiyu Wu, Zihui Gu, Zijia Zhu, Zijun Liu, Zilin Li, Ziwei Xie, Ziyang Song, Zizheng Pan, Zhen Huang, Zhipeng Xu, Zhongyu Zhang, and Zhen Zhang. Deepseek-r1: Incentivizing reasoning capability in llms via reinforcement learning, 2025.
- [10] John Schulman, Filip Wolski, Prafulla Dhariwal, Alec Radford, and Oleg Klimov. Proximal policy optimization algorithms, 2017.

- [11] Sergey Levine, Aviral Kumar, George Tucker, and Justin Fu. Offline reinforcement learning: Tutorial, review, and perspectives on open problems, 2020.
- [12] Scott Fujimoto, David Meger, and Doina Precup. Off-policy deep reinforcement learning without exploration, 2019.
- [13] Marcin Andrychowicz, Filip Wolski, Alex Ray, Jonas Schneider, Rachel Fong, Peter Welinder, Bob McGrew, Josh Tobin, Pieter Abbeel, and Wojciech Zaremba. Hindsight experience replay, 2018.
- [14] Adrien Ecoffet, Joost Huizinga, Joel Lehman, Kenneth O. Stanley, and Jeff Clune. Go-explore: a new approach for hard-exploration problems, 2021.
- [15] Jason Wei, Maarten Bosma, Vincent Y. Zhao, Kelvin Guu, Adams Wei Yu, Brian Lester, Nan Du, Andrew M. Dai, and Quoc V. Le. Finetuned language models are zero-shot learners, 2022.
- [16] Victor Sanh, Albert Webson, Colin Raffel, Stephen H. Bach, Lintang Sutawika, Zaid Alyafeai, Antoine Chaffin, Arnaud Stiegler, Teven Le Scao, Arun Raja, Manan Dey, M Saiful Bari, Canwen Xu, Urmish Thakker, Shanya Sharma Sharma, Eliza Szczechla, Taewoon Kim, Gunjan Chhablani, Nihal Nayak, Debajyoti Datta, Jonathan Chang, Mike Tian-Jian Jiang, Han Wang, Matteo Manica, Sheng Shen, Zheng Xin Yong, Harshit Pandey, Rachel Bawden, Thomas Wang, Trishala Neeraj, Jos Rozen, Abheesht Sharma, Andrea Santilli, Thibault Fevry, Jason Alan Fries, Ryan Teehan, Tali Bers, Stella Biderman, Leo Gao, Thomas Wolf, and Alexander M. Rush. Multitask prompted training enables zero-shot task generalization, 2022.
- [17] Tianzhe Chu, Yuexiang Zhai, Jihan Yang, Shengbang Tong, Saining Xie, Dale Schuurmans, Quoc V. Le, Sergey Levine, and Yi Ma. Sft memorizes, rl generalizes: A comparative study of foundation model post-training, 2025.
- [18] Daniel M. Ziegler, Nisan Stiennon, Jeffrey Wu, Tom B. Brown, Alec Radford, Dario Amodei, Paul Christiano, and Geoffrey Irving. Fine-tuning language models from human preferences, 2020.
- [19] Yun Luo, Zhen Yang, Fandong Meng, Yafu Li, Jie Zhou, and Yue Zhang. An empirical study of catastrophic forgetting in large language models during continual fine-tuning, 2025.
- [20] Suhas Kotha, Jacob Mitchell Springer, and Aditi Raghunathan. Understanding catastrophic forgetting in language models via implicit inference, 2024.
- [21] Heshan Fernando, Han Shen, Parikshit Ram, Yi Zhou, Horst Samulowitz, Nathalie Baracaldo, and Tianyi Chen. Mitigating forgetting in llm supervised fine-tuning and preference learning, 2025.
- [22] Wei Xiong, Jiarui Yao, Yuhui Xu, Bo Pang, Lei Wang, Doyen Sahoo, Junnan Li, Nan Jiang, Tong Zhang, Caiming Xiong, and Hanze Dong. A minimalist approach to llm reasoning: from rejection sampling to reinforce, 2025.
- [23] Youssef Mroueh. Reinforcement learning with verifiable rewards: Grpo's effective loss, dynamics, and success amplification, 2025.
- [24] Hanze Dong, Wei Xiong, Bo Pang, Haoxiang Wang, Han Zhao, Yingbo Zhou, Nan Jiang, Doyen Sahoo, Caiming Xiong, and Tong Zhang. Rlhf workflow: From reward modeling to online rlhf, 2024.
- [25] Douglas C. Crowder, Darrien M. McKenzie, Matthew L. Trappett, and Frances S. Chance. Hindsight experience replay accelerates proximal policy optimization, 2024.
- [26] Liang Wen, Yunke Cai, Fenrui Xiao, Xin He, Qi An, Zhenyu Duan, Yimin Du, Junchen Liu, Lifu Tang, Xiaowei Lv, Haosheng Zou, Yongchao Deng, Shousheng Jia, and Xiangzheng Zhang. Light-rl: Curriculum sft, dpo and rl for long cot from scratch and beyond, 2025.
- [27] Long Ouyang, Jeff Wu, Xu Jiang, Diogo Almeida, Carroll L. Wainwright, Pamela Mishkin, Chong Zhang, Sandhini Agarwal, Katarina Slama, Alex Ray, John Schulman, Jacob Hilton, Fraser Kelton, Luke Miller, Maddie Simens, Amanda Askell, Peter Welinder, Paul Christiano, Jan Leike, and Ryan Lowe. Training language models to follow instructions with human feedback, 2022.
- [28] An Yang, Anfeng Li, Baosong Yang, Beichen Zhang, Binyuan Hui, Bo Zheng, Bowen Yu, Chang Gao, Chengen Huang, Chenxu Lv, Chujie Zheng, Dayiheng Liu, Fan Zhou, Fei Huang, Feng Hu, Hao Ge, Haoran Wei, Huan Lin, Jialong Tang, Jian Yang, Jianhong Tu, Jianwei Zhang,

Jianxin Yang, Jiaxi Yang, Jing Zhou, Jingren Zhou, Junyang Lin, Kai Dang, Keqin Bao, Kexin Yang, Le Yu, Lianghao Deng, Mei Li, Mingfeng Xue, Mingze Li, Pei Zhang, Peng Wang, Qin Zhu, Rui Men, Ruize Gao, Shixuan Liu, Shuang Luo, Tianhao Li, Tianyi Tang, Wenbiao Yin, Xingzhang Ren, Xinyu Wang, Xinyu Zhang, Xuancheng Ren, Yang Fan, Yang Su, Yichang Zhang, Yingger Zhang, Yu Wan, Yuqiong Liu, Zekun Wang, Zeyu Cui, Zhenru Zhang, Zhipeng Zhou, and Zihan Qiu. Qwen3 technical report, 2025.

- [29] Karl Cobbe, Vineet Kosaraju, Mohammad Bavarian, Mark Chen, Heewoo Jun, Lukasz Kaiser, Matthias Plappert, Jerry Tworek, Jacob Hilton, Reiichiro Nakano, Christopher Hesse, and John Schulman. Training verifiers to solve math word problems, 2021.
- [30] Longhui Yu, Weisen Jiang, Han Shi, Jincheng Yu, Zhengying Liu, Yu Zhang, James T. Kwok, Zhenguo Li, Adrian Weller, and Weiyang Liu. Metamath: Bootstrap your own mathematical questions for large language models, 2024.
- [31] Lei Wang, Wanyu Xu, Yihuai Lan, Zhiqiang Hu, Yunshi Lan, Roy Ka-Wei Lee, and Ee-Peng Lim. Plan-and-solve prompting: Improving zero-shot chain-of-thought reasoning by large language models, 2023.
- [32] Yixin Ye, Zhen Huang, Yang Xiao, Ethan Chern, Shijie Xia, and Pengfei Liu. Limo: Less is more for reasoning, 2025.
- [33] Zhoujun Cheng, Haoyu Dong, Zhiruo Wang, Ran Jia, Jiaqi Guo, Yan Gao, Shi Han, Jian-Guang Lou, and Dongmei Zhang. Hitab: A hierarchical table dataset for question answering and natural language generation, 2022.

Contents of Appendix

A Limitations and Future Work	14
B Broader Impacts and Safeguards	14
C Detailed Settings of Experiments	15
C.1 Dataset Configurations	15
C.2 Model Configurations	16
C.3 Construction and Utilization of Offline Reasoning Data	16
C.4 Prompt and Output Format Design	17
C.5 Reward Design	18
C.6 Metric Design	18
C.7 Environment Setup	19
C.8 Details for K-step Parameter Settings Exploration	20
D Lessons Learned from Failed Attempts and Design Iterations	21
D.1 The Pitfalls of Integrating Online Rollouts into Supervised Fine-Tuning in Hybrid Actor	22
D.2 Offline Data as GRPO-Compatible Rollouts: A Negative Result	23
D.2.1 Variant I: Direct Injection of Expert Rollouts	23
D.2.2 Variant II: Self-Rewritten Expert Rollouts	23
D.3 Conclusion: Offline Rollouts Undermine GRPO Stability	24
D.4 Offline Data as Few-shots	24
D.5 Human Written or Synthetic Offline Data	25
D.6 Comparative Study of Hybrid Loss Integration Strategies	25
D.6.1 Design and Evaluation of Hybrid Learning Strategies	26
D.6.2 Analysis of Hybrid Actor Variants	27
D.7 Distillation or Hybrid? Choosing by Data Regime	27
E Soft Fusion over Hard Switching: A Unified Perspective on SuperRL versus SFT+RL	29

A Limitations and Future Work

Despite the strong empirical results of SuperRL, several limitations remain that point toward fruitful directions for future research.

Actor–Critic Integration Scope. Our current SuperRL framework fuses supervised and reinforcement signals solely at the actor level, leaving the critic architecture unchanged. This limits the potential benefits of supervision on value estimation, especially in reward-sparse settings where critic instability is a known issue. While the actor benefits from adaptive loss weighting, the critic may still suffer from high variance or misaligned value targets. Future work could explore critic-aware hybridization—such as incorporating auxiliary imitation-based value heads, distillation from teacher critics trained on demonstrations, or uncertainty-guided target shaping—to jointly stabilize actor and critic learning.

Static Fusion Strategy. The uncertainty-weighted hybrid loss in the Hybrid Actor in SuperRL provides a principled and adaptive mechanism for balancing objectives, but remains fixed across datasets once initialized. In practice, certain datasets (e.g., highly structured or low-noise) may admit more lightweight or specialized fusion strategies that require less computational overhead or training complexity. Designing dataset-aware or task-specific hybridization mechanisms—such as confidence-triggered SFT modulation or curriculum-guided loss annealing—could yield more efficient and tailored learning strategies.

Rule-Based Framework Design. The SuperRL currently employs a hard-coded, rule-based mechanism to estimate dataset difficulty and select training strategies in the Adaptive Switch. While effective in our experiments, this approach is coarse-grained and may fail to capture nuanced distinctions in task complexity or reward structure. In future work, we plan to replace this module with a learned policy selector that dynamically predicts the optimal training configuration based on early-stage learning signals (e.g., reward variance, KL divergence trends, early plateau detection). This direction may benefit from techniques in meta-learning, reinforcement curriculum learning, or Bayesian optimization.

Scalability and Efficiency. Although we demonstrate the broad applicability of SuperRL across multiple actor–critic algorithms and base models, its reliance on dual-loss computation and uncertainty learning introduces overhead in both compute and memory. Scaling the framework to very large models or long-horizon tasks may therefore require architectural optimizations such as parameter sharing across objectives, loss decoupling, or batch reweighting heuristics. Additionally, efficient parallelization strategies for joint SFT and RL processing are important for deployment at production scale.

In summary, while SuperRL provides a robust foundation for integrating supervised priors into reinforcement learning for language models, we believe further refinement of actor–critic design, adaptivity mechanisms, and system scalability will be crucial for advancing the field toward more generalizable and efficient hybrid training strategies.

B Broader Impacts and Safeguards

The proposed SuperRL framework introduces a new hybrid reinforcement learning strategy that integrates SFT loss into the actor’s update loop. This approach may carry several broader impacts, particularly in the context of increasingly capable and general-purpose language models. On the one hand, the improvements in convergence stability, sample efficiency, and generalization under sparse-reward conditions make this method attractive for domains where reinforcement learning has traditionally struggled. These include education, programming assistance, automated scientific discovery, and other settings where precise reasoning and data efficiency are critical. The reduced reliance on large volumes of reward-labeled data may also lower the entry barrier for fine-tuning smaller models in more constrained or specialized environments.

At the same time, as with many advances in RL and LLM training, potential concerns arise regarding misuse and unintended consequences. Enhanced reasoning capabilities may inadvertently be applied in domains such as persuasive content generation, misinformation synthesis, or manipulation of

human preferences—especially if downstream applications fail to incorporate adequate human oversight. Furthermore, the incorporation of supervised signals throughout training means that any biases embedded in the training corpus may persist or even be reinforced during policy updates, particularly if the model overfits to surface-level heuristics present in expert demonstrations.

It is also worth noting that while the hybrid loss improves stability, it does not guarantee robustness or fairness under distributional shifts. The method assumes access to high-quality expert data and reasonably aligned reward signals; in settings where these assumptions do not hold, model behavior may become unpredictable or brittle. In addition, the hybrid approach may make model attribution more difficult, as it intertwines supervised and reinforcement-driven behaviors during learning, complicating post hoc interpretation of model decisions.

We do not make specific claims regarding the societal or safety alignment of models trained under this framework. The practical implications of SuperRL—positive or negative—will ultimately depend on the nature of its application and the surrounding deployment context. Nonetheless, we believe that discussions around the responsible development and use of hybrid training frameworks are important and ongoing. Future research may benefit from more targeted evaluations of fairness, robustness, and transparency in hybrid optimization, especially as such techniques become more widely adopted in real-world systems.

C Detailed Settings of Experiments

C.1 Dataset Configurations

To rigorously evaluate SuperRL, we utilize six diverse datasets encompassing various reasoning challenges, from arithmetic problem-solving to complex symbolic logic and semi-structured data analysis. Below, we provide detailed descriptions of each dataset:

GSM8K is a benchmark dataset comprising 8,500 high-quality grade school math word problems, crafted by human problem writers. The dataset is divided into 7,500 training and 1,000 test examples. Each problem typically requires 2 to 8 steps to solve, involving basic arithmetic operations such as addition, subtraction, multiplication, and division. GSM8K serves as a standard for evaluating multi-step mathematical reasoning in language models.

MetaMathQA is a large-scale dataset containing 395,000 mathematical question-answer pairs. The dataset is generated by augmenting existing problems from GSM8K and MATH datasets, ensuring diversity and complexity in mathematical reasoning tasks. MetaMathQA aims to enhance the forward and backward reasoning capabilities of models across various mathematical domains, including algebra, geometry, and calculus.

PRM12K is a subset of the PRM800K dataset, focusing on mathematical problems. It consists of 12,000 samples, each accompanied by five different solution paths, encompassing both correct and incorrect answers. Unlike some filtered datasets, PRM12K retains all samples, providing additional columns to indicate the correctness of each solution. This structure makes it particularly suitable for preference learning and reward modeling tasks.

OpenR1-Math-220k is a comprehensive dataset designed for mathematical reasoning, comprising 220,000 math problems. Each problem is associated with two to four reasoning traces generated by the DeepSeek R1 model. The traces have been verified using tools like Math Verify and Llama-3.3-70B-Instruct, ensuring at least one correct reasoning path per problem. This dataset challenges models to understand and replicate complex reasoning processes.

LIMO (Less is More for Reasoning) is a benchmark that challenges the conventional belief that large datasets are necessary for effective reasoning. It contains only 817 meticulously curated training samples, yet models trained on LIMO demonstrate superior performance across multiple benchmarks. LIMO emphasizes the quality of training data over quantity, showcasing that complex reasoning abilities can be elicited with limited but well-structured examples.

HiTab is a dataset developed for question answering and natural language generation over hierarchical tables. It includes 3,597 tables and 10,686 QA pairs, sourced from statistical reports and Wikipedia pages. The tables exhibit complex hierarchical structures, and the dataset provides fine-grained annotations for entity and quantity alignment. HiTab poses significant challenges in numerical reasoning due to its hierarchical indexing and implicit semantic relationships.

Table 5: Benchmarks used in this study. “–” indicates the split is not officially provided.

Dataset	# Train	# Test	Task Type	Domain	License	Source
GSM8K [29]	7,473	1,319	Math word problems	Elementary math	MIT	Link
METAMATHQA [30]	395,000	–	Math QA	Mathematics	MIT	Link
PRM12K [31]	12,000	–	Programmatic reasoning	Mathematics	Apache 2.0	Link
LIMO [32]	817	–	Few-shot reasoning	Mathematics	MIT	Link
OPENR1-MATH-220K	220,000	–	Math reasoning	Mathematics	Apache 2.0	Link
HiTAB [33]	7,399	1,583	Hierarchical table QA	Statistics	C-UDA 1.0	Link

C.2 Model Configurations

To comprehensively evaluate SuperRL, we select a diverse set of open-source language models varying in size, architecture family, and training objectives. These models span three primary families: **Qwen2.5**, **LLaMA 3.x**, and **DeepSeek-R1 Distilled**. Below, we provide detailed descriptions of each:

Qwen2.5 Series is a family of autoregressive language models developed by Alibaba, instruction-tuned for a wide range of reasoning tasks. It offers multiple model sizes—0.5B, 1.5B, 3B, and 7B—allowing systematic exploration of scale effects. All models are licensed under Apache 2.0 and trained with a consistent architecture design and tokenizer, ensuring comparability across sizes.

DeepSeek-R1-Distill-1.5B is a distilled version of the original DeepSeek-R1 model, designed to preserve the reasoning capabilities of larger models while reducing computational overhead. It is instruction-tuned on diverse reasoning traces and optimized for both efficiency and generalization. This 1.5B model plays a key role in evaluating compact reasoning models.

LLaMA 3.x Series includes models from the LLaMA 3.1 and 3.2 releases by Meta, with community-instruct fine-tuning. We use the 1B and 3B models from LLaMA 3.2, and the 8B model from LLaMA 3.1. These models are known for their competitive instruction-following ability and are widely adopted in the community for downstream alignment tasks.

All model weights are publicly available under permissive licenses, enabling reproducible benchmarking. Table 6 summarizes the key properties of each model used in our experiments.

Table 6: Model configurations evaluated in our experiments.

Model	Parameters (B)	Family	License	Source
Qwen2.5-0.5B	0.5	Qwen2.5	Apache 2.0	Link
Qwen2.5-1.5B	1.5	Qwen2.5	Apache 2.0	Link
Qwen2.5-3B	3	Qwen2.5	Apache 2.0	Link
Qwen2.5-7B	7	Qwen2.5	Apache 2.0	Link
R1-Distill-1.5B	1.5	DeepSeek-R1	MIT	Link
Llama3.2-1B-Instruct	1	Llama 3.2	Llama 3 Community	Link
Llama3.2-3B-Instruct	3	Llama 3.2	Llama 3 Community	Link
Llama3.1-8B-Instruct	8	Llama 3.1	Llama 3 Community	Link

C.3 Construction and Utilization of Offline Reasoning Data

The offline SFT data utilized in SuperRL is derived from expert-annotated or high-quality model-generated reasoning traces. Many of the datasets we employ inherently contain rich, step-by-step problem-solving trajectories, serving as natural sources of offline supervision.

For instance, the GSM8K dataset provides detailed answer fields comprising multi-step reasoning chains and final solutions, making it directly suitable for use as SFT targets. Similarly, PRM12K offers both expert-annotated solutions and a substantial portion of high-quality, model-generated reasoning traces. We meticulously validate and include these generated traces in our SFT corpus when their final answers align with the correct labels.

LIMO, originally designed to study long-horizon mathematical reasoning, was explicitly structured to benefit from supervised learning. Its strong performance under SFT alone motivated our inclusion of LIMO in the hybrid training setting, leveraging its expert-annotated solutions as high-quality offline supervision signals.

In contrast, HiTab lacks annotated intermediate reasoning steps, which are crucial for supervised learning in our hybrid training framework. To address this, we generate synthetic reasoning trajectories using a large instruction-tuned model (e.g., Deepseek-R1), prompted to produce step-by-step justifications for each QA pair. We implement a stringent answer-filtering mechanism: only when the generated rationale’s final answer matches the ground-truth label is it accepted into the SFT corpus. This ensures high precision and prevents low-quality traces from corrupting training.

Implementation in VERL. Within the VERL framework, whose license is Apache License 2.0, we adopt a structured approach to integrate offline trajectories into the training pipeline:

- **Data Annotation and Storage:** Each data sample is augmented with an extra `info` field, encapsulating metadata such as the original question, the extracted or generated reasoning trajectory, and the target answer. This design ensures that auxiliary information is preserved alongside the primary data, facilitating downstream processing.
- **Custom Dataset Class:** We define a custom `Dataset` class that preprocesses the annotated data. This class is responsible for converting each entry into a standardized `DataProto` object. The `DataProto` includes tokenized inputs, loss masks for supervised targets, and auxiliary fields for logging and analysis. This modular design promotes flexibility and reusability across different training configurations.
- **Integration with Actor Module:** The `Actor` module accesses the preprocessed `DataProto` objects during training. By leveraging the structured information within each `DataProto`, the `Actor` can efficiently retrieve high-quality supervision signals, ensuring that the model benefits from the rich reasoning trajectories during optimization.

This integration strategy ensures that the offline trajectories are seamlessly incorporated into the hybrid optimization process, providing consistent behavioral priors and enhancing the model’s reasoning capabilities.

C.4 Prompt and Output Format Design

To promote interpretable and verifiable reasoning behavior, we adopt distinct prompting and output formatting strategies tailored to the model type.

Prompt Design. For both vanilla and structured-output models, we append a concise instruction—“Let’s think step by step and output the final answer in `boxed{}`.”—to the original problem description to encourage step-by-step reasoning and a clearly identifiable final answer.

For example:

Prompt: If you have 3 apples and you buy 2 more, how many do you have? Let’s think step by step and output the final answer in `boxed{}`.

For **vanilla models** without structured output conventions, the model is directly given the above prompt string. A typical output is:

```
We start with 3 apples. Buying 2 more gives us 3 + 2 = 5.  
The final answer is boxed{5}.
```

In contrast, for **structured-output models** (e.g., Qwen2.5-1.5B, DeepSeek-R1-Distill-Qwen-1.5B) that support chat-style prompting, we apply `apply_chat_template` to transform the prompt into a ChatML-formatted conversation. For instance:

```

<|im_start|>system
You are a helpful assistant.<|im_end|>
<|im_start|>user
If you have 3 apples and you buy 2 more, how many do you
have? Let's think step by step and output the final answer
in boxed{}.<|im_end|>
<|im_start|>assistant
<think>

```

Expected Model Output and Postprocessing. The output format likewise depends on the model’s interface and training. For structured-output models, the expected output includes special tags:

```

We start with 3 apples. Buying 2 more gives us 3 + 2 = 5.
Now let's output the final answer.</think>
<answer>The answer is boxed{5}</answer>

```

In this case, we apply tag-aware parsing during postprocessing:

- Extract the reasoning trace enclosed in `<think>` tags.
- Extract the final answer from within the `<answer>` tag, specifically the content of `boxed{}`.

For vanilla models, which do not include tags, we rely on regex-based postprocessing:

- Identify the reasoning portion as any content before the appearance of `boxed{}`.
- Parse the numerical answer from within `boxed{}`.

These model-aware prompt formatting and output parsing strategies ensure the consistent interpretation of model responses across evaluation and training pipelines. They also enable structured reward computation and answer matching for reinforcement learning optimization.

C.5 Reward Design

Given a model response y to input x , we compute the reward as a binary signal:

$$r(x, y) = \begin{cases} 1 & \text{if } \text{extract}(y) = y^{\text{gt}} \\ 0 & \text{otherwise} \end{cases}$$

where $\text{extract}(y)$ denotes the parsed answer obtained via model-specific extraction logic, and y^{gt} is the ground-truth answer.

To accommodate surface-form variations—especially prevalent in datasets such as LIMO and PRM12K—we incorporate a *canonicalization layer* in the reward computation. This module standardizes answer representations by:

- Normalizing numeric formats (e.g., converting fractions to decimals);
- Performing symbolic equivalence checks (e.g., $2x + 4$ vs. $4 + 2x$);
- Unifying variable names, units, or other context-specific notations.

If the canonicalized prediction matches any canonicalized gold reference, we assign a reward of 1.

As a fallback mechanism, when no delimiters (e.g., `\boxed{}`) are detected in the model output, we extract the last numerical span as a proxy for the final answer. All reward functions are implemented as deterministic, stateless modules to ensure reproducibility and compatibility with batched rollout evaluations in PPO and GRPO training pipelines.

C.6 Metric Design

We adopt **Exact Match (EM)** accuracy as the primary evaluation metric to assess model performance on reasoning tasks. A prediction is considered correct if the extracted answer exactly matches the ground-truth answer after normalization. This includes removing extraneous formatting, standardizing

numerical representations, and optionally applying symbolic simplification when applicable. EM offers a strict yet interpretable signal of end-to-end correctness, effectively capturing whether the model arrives at the correct final solution.

Compared to token-level metrics such as BLEU or ROUGE—which quantify n-gram overlap—EM is more aligned with the discrete nature of most reasoning tasks. Token-based metrics often tolerate superficial similarity while overlooking semantically crucial deviations (e.g., predicting 7.0 instead of 7.5), thus failing to penalize incorrect answers that appear linguistically similar. In contrast, EM enforces a high bar for correctness by requiring exact alignment with the reference answer.

To accommodate datasets with multiple valid reasoning paths or equivalent solutions—such as PRM12K and OpenR1—we extend EM to a *relaxed matching* scheme. Specifically, a prediction is marked as correct if it matches *any* of the acceptable reference answers after canonicalization. This allows for flexibility in surface forms (e.g., equivalent algebraic expressions or unit conversions) while preserving the core requirement of semantic equivalence.

In all cases, the normalization and canonicalization procedures used during EM evaluation are kept deterministic and model-agnostic to ensure reproducibility and fairness. This design choice ensures that the metric remains robust across diverse model architectures and output formats.

C.7 Environment Setup

All experiments are conducted within the `ver1` framework, a scalable actor–critic reinforcement learning platform tailored for optimizing language models. This framework serves as the foundation for our experimental setup, allowing us to implement and iterate on various training strategies. Our primary experiments utilize GRPO as the core reinforcement learning algorithm. However, to validate the general applicability of our uncertainty-weighted hybrid training framework, we also conduct comparative trials using PPO. The configurations, scripts and source code for these experiments are all developed and modified within the `ver1`. This includes the implementation of the GRPO and PPO algorithms, as well as the integration of the uncertainty-weighted hybrid training approach. The flexibility of the `ver1` enables us to seamlessly update and refine our methods, ensuring that our experiments are both robust and adaptable.

Our experimental scripts follow a unified and modular configuration framework designed to ensure consistency across all datasets and model backbones. This framework supports flexible adaptation, with minor adjustments made to accommodate variations in model scale (e.g., parameter count) and available computational resources (e.g., GPU memory capacity). By default, both the actor and critic are initialized from the same pretrained checkpoint. This shared initialization helps maintain stability in the early stages of training and ensures that policy updates build upon a consistent starting point. Unless otherwise noted, we train the entire model with full-parameter updates, rather than using techniques like partial tuning or adapters. To manage memory consumption during training, we enable gradient checkpointing, which trades off additional computation for significantly reduced memory usage. This is particularly important when training large models with long sequences or large batch sizes. To constrain policy drift and encourage stable learning, we apply KL divergence regularization between the current policy and a fixed reference policy. We use a low-variance KL formulation with a fixed regularization coefficient of 0.001, following prior work showing its effectiveness in language model fine-tuning.

We adopt a fixed learning rate of 1e-6 for all experiments, regardless of dataset or model size. This consistent setting simplifies hyperparameter tuning and facilitates fair comparisons across different tasks. The batch size is set to 32 by default, which provides a good balance between training stability and GPU memory efficiency. However, in data-scarce scenarios—such as the LIMO dataset, which contains relatively few high-quality training samples—we reduce the batch size to 8 to improve gradient quality and mitigate overfitting risks associated with small datasets. Each training run proceeds for 500 update steps, a schedule empirically chosen to ensure sufficient optimization while maintaining computational efficiency. To monitor progress and detect training instabilities early, we conduct model evaluation every 5 steps on a held-out validation set. At the end of training, we report the test-set performance at step 500 if the learning curve shows smooth convergence. In cases where the validation curve exhibits fluctuations or noise—typically due to reward sparsity or instability in policy gradients—we apply exponential moving average (EMA) smoothing to the score trajectory to

obtain a more reliable final evaluation metric. This ensures that our reported performance reflects the overall trend rather than being biased by momentary spikes or drops.

For rollout generation, we employ the vLLM backend, which enables efficient and scalable batched decoding with optimized GPU memory usage. Each prompt is decoded to produce five candidate responses, allowing for diverse sampling during training. To ensure stable runtime behavior, we cap GPU memory utilization at 40%. The decoding configuration adopts a stochastic sampling strategy with a temperature of 1.0, $\text{top-}k = -1$ (disabled), and $\text{top-}p = 1.0$, corresponding to unconstrained nucleus sampling. These settings encourage diverse yet coherent response generation from the model. We constrain the maximum sequence length—comprising both the input prompt and the generated output—to 2048 tokens. Prompts that exceed this limit are filtered out prior to generation, and any attempt to exceed the limit during decoding raises a truncation error. This strict enforcement helps maintain consistency and prevents the introduction of ambiguous or malformed training signals.

For dataset partitioning, we follow the original train/test splits provided by the benchmark for GSM8K and HiTAB, ensuring compatibility with prior work and fair comparison. For all other datasets containing more than 20,000 examples, we randomly subsample a total of 20,000 instances to reduce computational cost while maintaining representative coverage. The selected subset is then split into training and test sets using an 80/20 ratio. This standardized partitioning protocol facilitates consistent evaluation across diverse datasets with varying sizes and distributions.

All experiments are conducted on machines equipped with NVIDIA H100 GPUs. For most settings involving smaller models (e.g., 1-3B parameters), we utilize a 2-GPU configuration, which provides sufficient compute capacity for full-parameter training. In contrast, larger models (e.g., 7B and above) are trained in a distributed fashion using multiple nodes and GPUs. We construct multi-node clusters using Ray, a flexible framework for large-scale distributed computing. Once initialized, training is orchestrated through ver1’s distributed utilities, which support scalable actor-critic reinforcement learning with efficient inter-GPU communication and synchronization. The micro-batch size is fixed at 2 per GPU across all experiments, regardless of the number of nodes or model size. This setting balances memory usage and gradient estimation stability, especially under reinforcement learning with sparse rewards. To ensure a fair comparison across different training paradigms, we adopt a unified optimizer configuration—including learning rate, weight decay, and scheduler—for all methods: supervised-only (SFT), reinforcement learning-only (RL), sequential SFT+RL, and our proposed hybrid RL+SFT. This design isolates the effect of training strategies from confounding optimization differences.

For the SFT and SFT+RL baselines, we begin by fine-tuning the base model using the same training dataset, learning rate, and context length as in the RL-based training setups. The supervised fine-tuning is conducted for a total of 25 epochs, a duration chosen to ensure sufficient convergence without overfitting. Throughout training, we evaluate each epoch’s checkpoint on the held-out test set using greedy decoding, i.e., with temperature set to zero and no sampling. The checkpoint achieving the highest test-set performance is selected as the final SFT baseline. For the SFT+RL baseline, reinforcement learning is initialized from this best-performing SFT checkpoint. We then continue training the model under the same RL framework used in our hybrid method. The final performance of the SFT+RL model is reported based on the test-set score at the point where the learning curve reaches stable convergence. If the learning dynamics are noisy, we apply exponential moving average (EMA) smoothing to determine the final score in a robust manner.

C.8 Details for K-step Parameter Settings Exploration

We conduct ablation experiments using four initialization settings for the uncertainty weights: $\sigma_{pg} = 1, \sigma_{sft} = 1$, $\sigma_{pg} = 1, \sigma_{sft} = 0$, $\sigma_{pg} = 0, \sigma_{sft} = 1$, and our default $\sigma_{pg} = 0, \sigma_{sft} = 0$, denoted respectively as settings 11, 10, 01, and 00. We apply Hybrid training on GSM8k using QWen2.5-1.5B, and the Figure 4.5 show the evolution of scores on GSM8k and PRM12k as training steps increase.

We observe that on GSM8k, all four settings lead to similar performance trajectories, suggesting that this task is relatively insensitive to the relative weighting between policy gradient and imitation loss. The reward signal alone is strong enough to guide effective learning. In contrast, on PRM12k, the model collapses under the 10 setting ($\sigma_{pg} = 1, \sigma_{sft} = 0$), likely because the absence of supervision during initial training harms the model’s ability to generalize to more difficult PRM12k—whose distribution differs significantly and exhibits stronger structural regularities. The 00 setting ($\sigma_{pg} =$

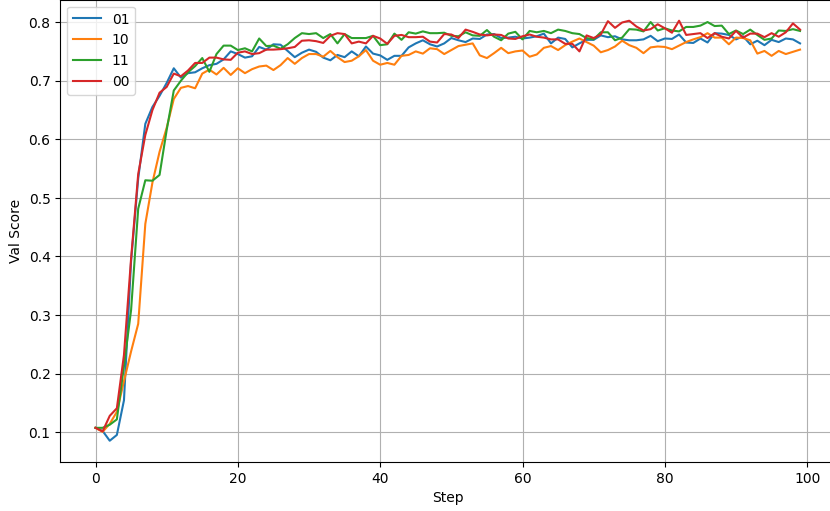


Figure 4: Validation Score on GSM8k When Trained on GSM8k Using Different Initial Strategies

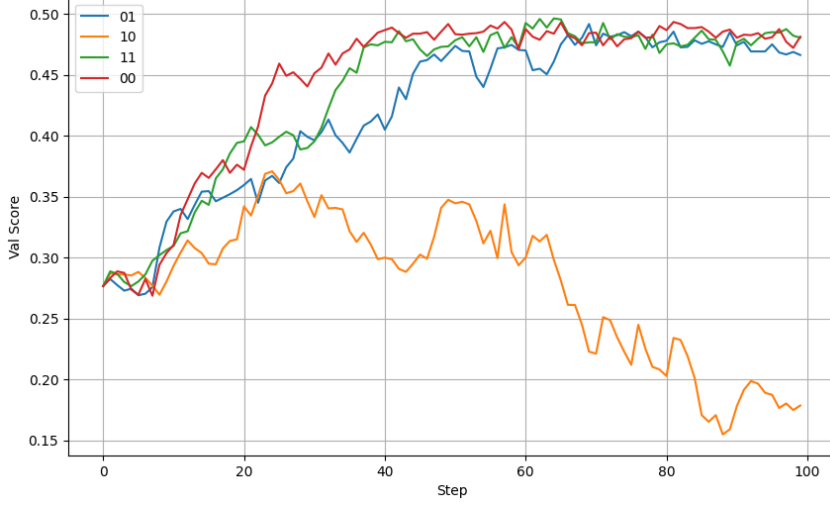


Figure 5: Val Score on PRM12k When Trained on GSM8k Using Different Initial Strategies

$0, \sigma_{sft} = 0$) achieves the best performance across both tasks, indicating that assigning strong and balanced weights to both the policy gradient and imitation losses at the beginning of training contributes to effective exploration and generalization.

To compute the average reward within different step ranges and the number of reward increases across the first k steps, we conduct 5 independent runs on GSM8k, MetaMath, PRM12k, OpenR1, and HiTab datasets. The batch size is varied across $\{16, 32, 64, 128, 256\}$. For the LIMO dataset, due to its smaller data volume, we perform 10 independent runs with a batch size of 8.

The following table shows representative examples over the first 10 RL steps using QWen2.5-1.5B trained with GRPO on GSM8k and HiTab. Each entry reports the average reward at a specific step, along with the total number of increases between adjacent steps.

D Lessons Learned from Failed Attempts and Design Iterations

Throughout the development of SuperRL, we explored a range of alternative strategies aimed at improving data efficiency and stability in RL for language models. A key motivating principle behind

Dataset	Step1	Step2	Step3	Step4	Step5	Step6	Step7	Step8	Step9	Step10	increase_num	recent_avg_reward
GSM8K	0.0617	0.0570	0.0828	0.1305	0.1820	0.2398	0.3148	0.3695	0.4609	0.4984	10	0.2397
HiTab	0.0008	0.0008	0.0023	0	0	0	0	0	0	0	1	0.0031

Table 7: Step-wise average reward during the first 10 RL updates on GSM8K and HiTab using QWen2.5-1.5B ($batch_size = 256$). Steps are split into two blocks for compact readability.

Table 8: On-Policy Evaluation Results on LIMO (Rollout-to-SFT)

Run Name	Final Score	Min Score	Max Score
Qwen2.5-1.5B_20250502	0.000	0.000	0.043
Qwen2.5-1.5B_20250501	0.000	0.000	0.042
Qwen2.5-1.5B_20250430	0.000	0.000	0.018

our early design iterations was to fully leverage existing supervision data within the RL training loop, regardless of whether it was collected off-policy or generated dynamically. This led us to investigate several hybrid approaches that sought to maximize the utility of available data across both supervised and reinforcement learning signals. Despite their conceptual appeal, many of these attempts failed to yield meaningful improvements, and in some cases, actively degraded performance. Below, we summarize the most instructive failures.

D.1 The Pitfalls of Integrating Online Rollouts into Supervised Fine-Tuning in Hybrid Actor

We explored an on-policy training strategy that integrates supervised learning directly Hybrid Actor by extracting learning signals from rollout responses(for GRPO algorithm). Unlike naive self-imitation, our method uses a reward-aware filtering mechanism: rollout responses are adopted as supervision targets only if they receive non-zero rewards; otherwise, the model reverts to offline expert-annotated responses. This allows the training signal to be dynamically chosen based on the quality of exploration outcomes. This mechanism enables the actor to optimize toward both policy improvement and imitation from valid behavior traces.

Despite the theoretical appeal of this formulation, its performance on reward-sparse benchmarks was consistently poor. As shown in Table 8, all variants of this reward-aware rollout-to-SFT approach achieved near-zero test scores on LIMO, a dataset characterized by complex multi-step reasoning and weak reward density.

Experimental Results. Despite its theoretical appeal, this rollout-to-SFT strategy failed to yield robust generalization in practice. As summarized in Table 8, all evaluated runs on the LIMO benchmark—representing complex, long-horizon reasoning tasks—collapsed to near-zero accuracy. This result holds across variations in random seed, training duration, and log-sigma scheduling.

Generalization Across Datasets. This failure pattern is not unique to the LIMO dataset. Across other reasoning benchmarks such as PRM12K, OpenR1, and HiTab, we observed similarly unstable training dynamics under the rollout-to-SFT paradigm. In some cases, such as PRM12K, the model exhibits a short-lived improvement in validation accuracy during early training, only to collapse irreversibly in later stages—indicative of an overfitting loop to spurious patterns in reward-positive trajectories. In others, including OpenR1 and HiTab, the model degrades steadily throughout training, failing to extract any durable learning signal from the reward-conditioned responses. Regardless of the specific trajectory, all runs eventually converge to near-zero accuracy, further affirming the brittleness of this approach in sparse or deceptive reward landscapes.

Failure Analysis. We identify several factors contributing to this consistent collapse. First, the strategy relies on the current policy to generate both inputs and supervision targets, which introduces a strong confirmation bias—especially problematic when rewards are sparse or noisy. The model reinforces its own suboptimal behavior without sufficient external correction, leading to overfitting on early or lucky successes. Second, since reward filtering allows only high-reward responses to propagate gradients, the effective batch size of learning signals becomes highly unstable and often too small for reliable policy updates. Third, the fallback to offline supervision in zero-reward cases introduces distributional mismatch between positive and negative samples, creating an inconsistent optimization target that destabilizes convergence. Finally, by tightly coupling exploration and

imitation in an on-policy loop, the model becomes more susceptible to cascading errors—where minor deviations early in training can quickly spiral into mode collapse under the compounding effects of self-reinforcement.

Collectively, these findings suggest that while reward-aware rollout-to-SFT is conceptually appealing for integrating exploration and learning, its naive implementation fails to provide a stable or scalable training signal in practice—particularly under the reward sparsity and multi-step dependencies typical of reasoning-centric tasks.

D.2 Offline Data as GRPO-Compatible Rollouts: A Negative Result

To investigate the potential of incorporating static expert supervision within GRPO training, we augment each sampled prompt by treating expert-annotated responses as auxiliary rollouts. Concretely, for every on-policy prompt sampled during training, the corresponding offline trajectory is injected into the GRPO buffer with its reward computed via a task-specific metric (e.g., exact match). These expert rollouts coexist with policy-generated samples, contributing to the surrogate loss and gradient updates. This design aims to regularize policy optimization and accelerate convergence by leveraging high-quality behavioral signals.

Empirical Collapse. Despite these motivations, both rollout-injection variants led to catastrophic learning failure: validation accuracy declined consistently throughout training, indicating that static expert rollouts destabilized optimization and accelerated mode collapse.

D.2.1 Variant I: Direct Injection of Expert Rollouts

This variant treats offline expert trajectories as if they were on-policy samples from the current policy π_θ , directly incorporating them into the GRPO buffer for joint optimization. At each training step, we sample a batch of expert trajectories $(x_e, y_e) \sim \mathcal{D}_{\text{expert}}$, assign rewards $r(x_e, y_e)$ based on task-specific metrics, and compute the mixed surrogate loss:

$$\mathcal{L}_{\text{mixed}} = \mathbb{E}_{(x, y) \sim \pi_\theta} [w(x, y) \cdot \log \pi_\theta(y|x)] + \lambda \cdot \mathbb{E}_{(x_e, y_e) \sim \mathcal{D}_{\text{expert}}} [r(x_e, y_e) \cdot \log \pi_\theta(y_e|x_e)], \quad (1)$$

where the first term corresponds to preference-weighted GRPO rollouts, and the second term injects expert supervision weighted by scalar λ .

Observed Failure. This strategy consistently degraded performance across all benchmarks (e.g., LIMO, HiTab), slowing convergence and increasing KL divergence relative to both pure GRPO and reward-aware rollout-to-SFT methods. We attribute this to *distributional mismatch*: expert trajectories (x_e, y_e) are not sampled from π_θ , violating GRPO’s on-policy assumption and introducing high-variance gradients. As a result, the policy oscillates between chasing unreachable expert targets and reinforcing suboptimal behaviors. This is reflected in elevated KL divergence:

$$\text{KL}(\pi_\theta \| \pi_{\text{ref}}) = \mathbb{E}_x \left[\sum_y \pi_\theta(y|x) \log \frac{\pi_\theta(y|x)}{\pi_{\text{ref}}(y|x)} \right], \quad (2)$$

signaling instability and misalignment with the initial reference distribution. Furthermore, static expert rollouts fail to adapt to the evolving policy’s exploration frontier, providing little guidance in unexplored regions of the solution space.

D.2.2 Variant II: Self-Rewritten Expert Rollouts

To address the distributional mismatch, we introduce a *self-rewrite* mechanism wherein expert responses are reformulated by the current policy to ensure alignment with its own distribution. Given $(x_e, y_e) \sim \mathcal{D}_{\text{expert}}$, we prompt π_θ to generate a rewritten response $\hat{y}_e \sim \pi_\theta(\cdot|x_e, y_e)$ that is semantically equivalent to y_e . The rewritten trajectory (x_e, \hat{y}_e) is assigned the same reward as the original expert response, yielding the loss:

$$\mathcal{L}_{\text{rewrite}} = \mathbb{E}_{(x, y) \sim \pi_\theta} [w(x, y) \cdot \log \pi_\theta(y|x)] + \lambda \cdot \mathbb{E}_{(x_e, \hat{y}_e) \sim \pi_\theta(\cdot|x_e, y_e)} [r(x_e, \hat{y}_e) \cdot \log \pi_\theta(\hat{y}_e|x_e)]. \quad (3)$$

Observed Failure. While distributional alignment is improved, this method failed to yield performance gains. Rewritten responses often diverged semantically from expert outputs, especially in multi-step reasoning tasks, introducing *semantic drift*. Assigning expert-level rewards $r(x_e, \hat{y}_e) = r(x_e, y_e)$

Table 9: Few-shot Prompting Performance with **Random Selection** (Qwen2.5-1.5B, GRPO)

Dataset	Vanilla	1-shot (Random)	3-shot (Random)	Best (Random)	Gain	Observation
GSM8K	0.755	0.747	0.745	Vanilla	-0.010	Few-shots degrade performance
MetaMath	0.814	0.793	0.8255	3-shot	+0.011	Faster convergence; slight gain
PRM12K	0.505	0.480	0.5057	3-shot	+0.007	Slight gain
LIMO	0.018	0.018 → 0	0.018 → 0	None	Collapse	All models collapse to 0

to imperfect rewrites led to reward misalignment:

$$\mathbb{E}[r(x_e, \hat{y}_e)] < r(x_e, y_e), \quad \text{but used reward } \approx r(x_e, y_e). \quad (4)$$

This misalignment inflated value predictions and reinforced spurious reasoning paths, resulting in cumulative confirmation bias and unstable convergence.

D.3 Conclusion: Offline Rollouts Undermine GRPO Stability

Our findings reveal that treating offline trajectories as GRPO-compatible rollouts—either directly or via self-rewriting—fails to improve and often degrades performance. These strategies violate GRPO’s on-policy assumptions and introduce high-variance or semantically misaligned gradients. We conclude that more principled methods are needed to bridge the gap between static supervision and dynamic exploration without compromising the stability of reinforcement learning updates.

D.4 Offline Data as Few-shots

To more effectively leverage the information contained in high-quality offline data, we explored augmenting the original prompt by prepending additional exemplars drawn from the same supervised dataset. These few-shot exemplars, comprising other question-solution pairs, are intended to serve as implicit guidance. By exposing the model to a wider range of reasoning patterns, we aim to enhance its generalization capabilities.

We explored three selection strategies for constructing these few-shot demonstrations: **Random Selection**: Randomly sample one or more exemplars from the SFT dataset without conditioning on the current prompt. **Prompt Similarity**: Retrieve exemplars whose questions are semantically similar to the target prompt, based on embedding-based similarity. **Solution Similarity**: Select exemplars whose solutions are structurally or semantically similar to the expert solution of the target prompt.

For each strategy, we varied the number of exemplars included in the prompt (one vs. three) to test whether increasing few-shot context leads to measurable improvements.

Empirical Observations. Despite the intuitive appeal of enriching the prompt with related examples, none of the strategies consistently outperformed the base model across benchmarks. The effectiveness of few-shot augmentation was highly variable: while minor gains were observed on specific reasoning-centric datasets such as MetaMath and PRM12K, performance degraded or remained stagnant on others, including GSM8K and LIMO. Notably, LIMO exhibited complete collapse under few-shot augmentation, echoing similar failure patterns seen in other unstable training regimes.

We performed extensive evaluations using the **Random Select** strategy across four datasets, while the **Prompt Similarity** and **Solution Similarity** strategies were validated on a subset due to computational constraints. Nevertheless, all methods displayed consistent patterns: no significant improvement was achieved over the vanilla setting, and the inclusion of static exemplars occasionally introduced additional variance or learning instability. Crucially, none of the approaches achieved the type of meaningful gains observed under our proposed hybrid training strategy, which dynamically balances supervised and policy gradient objectives.

In summary, our findings highlight the limitations of offline few-shot augmentation as a plug-and-play solution for improving GRPO training. The static nature of these exemplars, combined with potential mismatches in reasoning complexity or style, undermines their utility as general-purpose inductive scaffolds. While few-shot prompting may offer minor benefits in specific cases, it fails to deliver consistent performance gains and does not constitute a reliable substitute for hybrid or dynamically supervised training methods.

Table 10: Comparison of Human-written vs. Synthetic Solutions on PRM12K (Qwen2.5-1.5B, GRPO)

Method	Final Accuracy	Observation
Vanilla	0.49	Strong baseline without hybridization
Hybrid(Synthetic Data)	0.475	Slow start, eventually catches up
Hybrid(Synthetic Data)	0.504	Fastest convergence and best final score
Hybrid(Human-written Data)	0.482	More stable early-stage learning

D.5 Human Written or Synthetic Offline Data

To further examine the impact of solution provenance on policy learning under GRPO, we conducted targeted experiments on the PRM12K dataset, which uniquely provides two types of reference solutions per instance: a standard solution and several model-generated (synthetic) solutions. This dual annotation enables a controlled comparison between high-quality manual demonstrations and LLM-synthesized reasoning traces, which may vary in logical depth and fluency.

We implemented and evaluated several hybrid training variants that leverage these distinct solution types under our SFT-RL hybrid framework. The baseline (**Vanilla**) uses no hybridization and serves as a pure GRPO control. We then compared two hybrid configurations: one incorporating human-written solutions (**Hybrid-Human**), and another substituting in synthetic solutions from the dataset (**Hybrid-Synthetic**). Additionally, a per-step cosine-weighted hybrid approach was tested to assess the influence of reward shaping with respect to solution type.

The results in Table 10 suggest that both human-written and synthetic solutions can be effectively leveraged within our hybrid SFT-RL training framework. Compared to the **Vanilla** baseline (0.49), all hybrid variants exhibit comparable or improved performance, indicating that incorporating offline solutions—regardless of provenance—provides additional learning signal beneficial for policy optimization.

Notably, while the best-performing configuration utilizes synthetic data (0.504), the overall differences between human and synthetic variants remain modest. The **Hybrid (Human-written)** model achieves 0.482, and both variants using **Hybrid (Synthetic)** data fall within a similar performance band. This outcome suggests that model-generated solutions, despite potential imperfections, can approximate the utility of high-quality human annotations in guiding learning—especially when training is augmented with appropriate reward signals.

These findings challenge the assumption that human-written demonstrations are categorically superior for hybrid learning. Instead, they highlight the practical viability of synthetic solutions, which are more scalable to obtain in real-world settings. The relatively small performance gap also opens the door to future improvements through better filtering, weighting, or mixture modeling over solution sources.

Implications. These results underscore a practical advantage for scalable deployment: in many real-world scenarios, high-quality human-written data may be scarce or prohibitively expensive to collect. Our findings suggest that it is feasible to substitute such data with model-generated (synthetic) solutions—especially when integrated into training via techniques like SuperRL. This opens up a promising path for applying our method in low-resource domains, enabling policy learning from weaker yet abundant supervision sources. Further gains may be achieved by coupling this approach with strategic data curation methods such as solution filtering, reward-weighted sampling, or mixture-of-expert style routing over solution types.

D.6 Comparative Study of Hybrid Loss Integration Strategies

We investigate three distinct designs for hybrid optimization between policy gradients and supervised fine-tuning, aiming to exploit the complementary strengths of exploration and imitation. These variants differ in how they balance PPO loss (\mathcal{L}_{PPO}) and SFT loss (\mathcal{L}_{SFT}), and in how the mixing weights are learned and applied.

Table 11: LIMO Final Scores of Hybrid Actor Variants (Qwen2.5-1.5B)

Category	Method (Run)	Final Score	Trend
HYBRID LOG-SIGMA	Run 1	0.061	Improves steadily
	Run 2	0.058	Slightly fluctuating
	Run 3	0.060	Stable high
HYBRID THETA (α -weighted)	Run 1	0.019	Slow rise
	Run 2	0.017	Plateaus early
	Run 3	0.018	Fluctuates
HYBRID PER-STEP	Run 1	0.013	Collapse after peak
	Run 2	0.011	Fluctuating low
	Run 3	0.010	Declines continuously

D.6.1 Design and Evaluation of Hybrid Learning Strategies

To effectively balance SFT and RL objectives during actor training, we explore three hybrid optimization strategies that integrate both signals with different weighting mechanisms. Below, we present each design’s formulation and underlying rationale, followed by a comparative analysis on the GAIR/LIMO benchmark.

Hybrid Log-Sigma (Uncertainty-Based Weighting). This method introduces two independent learnable log-variance parameters, $\log \sigma_{\text{pg}}$ and $\log \sigma_{\text{sft}}$, to dynamically reweight the PPO loss \mathcal{L}_{PPO} and SFT loss \mathcal{L}_{SFT} . The total hybrid loss is given by:

$$\mathcal{L}_{\text{total}} = \exp(-2 \log \sigma_{\text{pg}}) \cdot \mathcal{L}_{\text{PPO}} + \exp(-2 \log \sigma_{\text{sft}}) \cdot \mathcal{L}_{\text{SFT}} + \log \sigma_{\text{pg}} + \log \sigma_{\text{sft}}$$

This formulation follows the uncertainty weighting paradigm proposed by Kendall et al. (2018), where the log-variance terms both modulate gradient scaling and regularize the optimization process. It allows the model to autonomously learn which objective to prioritize at each stage of training, adapting to dynamic gradient magnitudes and learning phases. Empirically, this method achieves the most stable training and best final performance on LIMO.

Hybrid Theta (α -Weighted Convex Combination). In this variant, a single scalar parameter α governs the mixing ratio between PPO and SFT losses via a sigmoid transformation:

$$w_{\text{pg}} = \sigma(\alpha), \quad w_{\text{sft}} = 1 - w_{\text{pg}}, \quad \mathcal{L}_{\text{total}} = w_{\text{pg}} \cdot \mathcal{L}_{\text{PPO}} + w_{\text{sft}} \cdot \mathcal{L}_{\text{SFT}}$$

The weights are constrained to form a convex combination, ensuring bounded influence from each loss term. Although simpler and easier to optimize, this approach lacks the fine-grained adaptivity of uncertainty-based methods. It struggles to respond to non-stationary gradients and therefore performs moderately in terms of stability and final score.

Hybrid Per-Step (Sequential Log-Sigma). This design decouples PPO and SFT into two consecutive optimization steps per batch. After completing the PPO update, an additional SFT step is performed using samples containing reference answers. The SFT objective is scaled by a log-variance parameter:

$$\mathcal{L}_{\text{SFT}}^{\text{weighted}} = \exp(-2 \log \sigma_{\text{sft}}) \cdot \mathcal{L}_{\text{SFT}} + \log \sigma_{\text{sft}}$$

While modular and implementation-friendly, this approach suffers from gradient inconsistency across updates. Since PPO and SFT gradients are applied separately, the optimization trajectory becomes unstable. Moreover, supervision is only introduced after the PPO step, reducing its effectiveness in guiding exploration. As a result, training frequently collapses or fails to converge stably.

Experimental Results on GAIR/LIMO. As shown in Table 11, the Hybrid Log-Sigma variant significantly outperforms the others on both final accuracy and stability metrics. The uncertainty-

weighted joint loss leads to smoother training dynamics and better generalization. In contrast, the α -weighted Hybrid Theta variant converges more slowly and achieves a lower final score. The sequential Hybrid Per-Step strategy performs the worst, suffering from frequent instability and collapse.

D.6.2 Analysis of Hybrid Actor Variants

We conduct a comprehensive evaluation of three hybrid actor designs on the LIMO benchmark to assess their stability and effectiveness under long-horizon reasoning tasks. As shown in Table 11, HYBRID LOG-SIGMA outperforms the other two variants across all metrics. Its final scores remain consistently high (0.060–0.061), with learning curves that are either steadily improving or stably maintained throughout training. In contrast, HYBRID THETA and HYBRID PER-STEP display marked signs of instability, with final scores falling below 0.02 and clear signs of collapse or early stagnation.

Hybrid Log-Sigma. This variant exhibits the most reliable optimization behavior. Its performance stability suggests that the dynamic weighting mechanism, which adjusts the balance between SFT and RL losses based on task difficulty and learning dynamics, effectively prevents either objective from dominating. Such adaptability is particularly critical in LIMO, where reasoning depth and reward sparsity fluctuate significantly across samples. The model learns to prioritize supervised signals early on and gradually shifts toward reward-driven fine-tuning, enabling smooth convergence without degrading performance.

Hybrid Theta. In contrast, the fixed-coefficient weighting used in this variant fails to accommodate the evolving balance between imitation and exploration. When the weight on SFT is too strong, the model struggles to learn from reward signals, leading to early saturation. Conversely, when RL is overweighted, learning becomes unstable due to reward sparsity. This rigidity in balancing objectives likely explains the plateaued or erratic learning curves observed across all three runs, with final scores ranging only from 0.017 to 0.019. None of the runs show significant late-stage improvement.

Hybrid Per-Step. This variant performs the worst across the board. By applying the hybrid loss at every generation step, it exposes the model to highly localized and often conflicting gradient signals between the SFT objective (which emphasizes sequence-level coherence) and the RL signal (which varies stochastically across steps). This fine-grained interference introduces high optimization variance, especially harmful on tasks like LIMO that require multi-step planning and semantic alignment. The result is catastrophic instability: one run collapses shortly after peaking, while others show continuous degradation, with final scores dropping to 0.010–0.013.

Conclusion. Among the three variants, only HYBRID LOG-SIGMA avoids collapse and achieves stable high performance on LIMO. Its dynamic loss weighting provides the flexibility required to navigate the complex trade-offs inherent in hybrid training. The empirical trends strongly support that principled uncertainty-based balancing is crucial for successful integration of SFT and RL signals, especially on benchmarks requiring compositional reasoning.

D.7 Distillation or Hybrid? Choosing by Data Regime

While our SuperRL demonstrates strong performance on small, high-quality datasets, recent distillation-based approaches—such as Deepseek-R1-Distill often surpass our results when ample high-quality offline data from different aspects are available. In particular, on the LIMO benchmark, the best R1-Distill variant achieves higher final exact-match accuracy, at the expense of substantially greater data and computation requirements.

Marginal Gains on Stronger Models. On the stronger R1-Distill-1.5B backbone, our Hybrid method yields modest but consistent improvements. Specifically, the accuracy on GSM8K rises from 74.5% to 76.3% (+1.8 percentage points), on PRM12K from 54.8% to 55.8% (+1.0 percentage points), and on LIMO from 30.0% to 31.2% (+1.2 percentage points). These small absolute gains reflect the diminishing returns when distillation has already imbued the model with high-quality reasoning traces. Notably, the improvements are relatively minor compared to the substantial gains observed on weaker models, highlighting the diminishing effectiveness of additional optimization techniques on already well-performing models.

Table 12: Exact-Match Accuracy on GSM8K, PRM12K, and LIMO using R1-Distill-1.5B and Qwen2.5-1.5B

Method (Run)	GSM8K		PRM12K		LIMO	
	R1-Distill	Qwen2.5	R1-Distill	Qwen2.5	R1-Distill	Qwen2.5
Vanilla	0.745	59.7%	0.548	26.7%	0.300	1.2%
Hybrid (Run-1)	0.759	77.0%	0.553	14.0%	0.312	2.6%
Hybrid (Run-2)	0.763	74.7%	0.558	35.1%	0.295	6.9%
Hybrid (Run-3)	0.748	70.0%	0.540	33.0%	0.289	1.8%
Hybrid (Run-4)	0.749	74.7%	0.543	47.7%	0.295	3.0%

Substantial Improvements on Weaker Backbones. By contrast, when applied to the base Qwen-1.5B model, Hybrid unlocks far larger relative improvements over its vanilla SFT performance. The accuracy on GSM8K jumps from 59.7% to 77.0% (+17.3 percentage points), on PRM12K from 26.7% to 35.1% (+8.4 percentage points), and on LIMO from 1.2% to 6.9% (+5.7 percentage points). This demonstrates Hybrid’s ability to rescue underperforming backbones by interleaving SFT and RL, even without a separate distillation teacher. The significant gains on weaker models underscore the effectiveness of Hybrid in enhancing reasoning capabilities where traditional SFT alone falls short.

Dataset Difficulty and Regime Selection. Despite these gains, absolute performance on the hardest dataset (LIMO) remains low (<32%) for both models, underscoring that Hybrid alone cannot substitute for the rich, multi-step traces distilled in R1-Distill. In data-rich, multi-domain settings, a dedicated multi-round SFT+RL (distillation) pipeline is justified by the higher asymptotic accuracy. However, in single-dataset or low-resource scenarios—where collecting extensive expert traces is impractical—Hybrid offers superior sample efficiency and robust gains, making it the preferable choice.

Why R1-Distill-1.5B Excels. The R1-Distill-1.5B variant attains its strong performance by first leveraging a high-capacity teacher model to generate rich, multi-step reasoning traces over a large, heterogeneous corpus of problems. These synthetic expert traces are then used in a multi-stage distillation pipeline: an initial supervised fine-tuning (SFT) phase to bootstrap reasoning capabilities, followed by on-policy reinforcement learning (RL) with a behavior-cloned policy as initialization. This two-phase approach both transfers the teacher’s structured reasoning patterns and refines them under the true task reward, yielding substantial gains when the distillation corpus is sufficiently large and diverse. The effectiveness of R1-Distill-1.5B is particularly pronounced in settings with abundant data and computational resources, where the model can fully leverage the high-quality reasoning traces generated by the teacher model.

Utility of Our Hybrid Method. By contrast, our SuperRL hybrid method interleaves SFT and RL updates at every optimization step using an uncertainty-weighted loss, avoiding the need for separate distillation and RL phases. This unified fusion enables stable learning even when only a modest amount of high-quality reasoning data is available. As Table 12 demonstrates, Hybrid matches or nearly matches R1-Distill performance on GSM8K and PRM12K under constrained data budgets, while requiring significantly less compute and no external distillation teacher. The Hybrid method’s ability to achieve comparable performance with fewer resources highlights its efficiency and adaptability in resource-limited environments.

Data Regime Considerations. When abundant multi-domain reasoning traces can be collected or synthesized, a dedicated distillation pipeline (i.e., multi-round SFT followed by RL) can push base models beyond Hybrid’s plateau, as seen on LIMO. However, in single-dataset or low-resource settings—where acquiring large, diverse expert traces is impractical—our single-stage Hybrid approach delivers superior sample efficiency and robustness. Thus, practitioners should favor distillation-based SFT+RL when ample data and compute are available, but rely on Hybrid to unlock reasoning gains in the small-data regime. The choice between these methods should be guided by the availability of resources and the specific characteristics of the dataset and task at hand.

E Soft Fusion over Hard Switching: A Unified Perspective on SuperRL versus SFT+RL

A central challenge in aligning large language models (LLMs) with desired behaviors lies in how to effectively combine supervised fine-tuning (SFT) and reinforcement learning (RL). While both paradigms contribute valuable learning signals—SFT offering human-aligned supervision and RL enabling optimization toward long-term utility—the way these signals are integrated significantly affects the model’s learning stability, generalization ability, and sample efficiency.

The traditional SFT+RL framework adopts a hard two-stage approach. During the first stage, the model is trained to imitate expert demonstrations using SFT, thereby anchoring the policy to safe and interpretable behaviors. Once a strong imitation prior is established, the second stage introduces RL to optimize a reward signal derived from task metrics or preference models. Although intuitive and easy to implement, this sequential strategy suffers from three core limitations. First, the abrupt shift in training objectives often leads to instability and catastrophic forgetting of prior knowledge. Second, the strong imitation prior may reduce the model’s willingness to explore behaviors that deviate from demonstrations, even when such behaviors yield higher rewards. Third, in the absence of balancing supervision, the RL phase can over-optimize to flawed or narrow reward functions, thereby harming generalization.

In contrast, SuperRL adopts a soft fusion strategy, where SFT and RL signals are blended within each training iteration rather than staged sequentially. Instead of viewing imitation and exploration as isolated phases, SuperRL treats them as co-evolving learning signals, optimized jointly throughout training. The relative importance of each objective is dynamically adjusted based on their estimated uncertainty, allowing the learning system to flexibly prioritize the more informative signal at each point in training. This formulation offers several benefits. By maintaining the influence of SFT across all steps, SuperRL prevents sharp behavioral drift and promotes smooth policy evolution. Its uncertainty-weighted mechanism enables dynamic rebalancing, allowing the model to emphasize exploration when confident and revert to supervision when uncertain. Furthermore, this joint optimization encourages the model to reconcile imitation and reward-driven adaptation, ultimately improving its ability to generalize to out-of-distribution settings.

Rather than treating hard switching and soft fusion as binary opposites, we consider them as two ends of a continuous spectrum. Hard switching may be advantageous in environments where demonstrations are accurate and dense, and the reward function is well-aligned with those demonstrations. However, in more complex or underspecified settings—such as open-ended reasoning tasks, preference-based generation, or safety-critical applications—the rigidity of hard switching becomes a liability. Here, soft fusion mechanisms like SuperRL provide better flexibility and robustness by continuously adjusting to evolving training signals and conflicting supervision sources.

A central innovation of SuperRL is the uncertainty-weighted hybrid actor, which assigns adaptive weights to SFT and RL loss terms based on their reliability. This allows the model to down-weight noisy or misleading signals and focus on gradients that offer higher expected utility. Such a mechanism is especially valuable when either the reward function or the demonstrations are partial, evolving, or domain-dependent. It helps mitigate destructive interference between incompatible objectives, improve sample efficiency under sparse rewards, and preserve human-aligned behaviors without limiting the model’s capacity to explore novel solutions.

Despite its strengths, the soft fusion strategy is not without limitations. First, optimizing SFT and RL objectives jointly may lead to conflicting gradients, resulting in diluted or unstable updates if neither signal dominates. Second, the method’s success hinges on the accuracy of the uncertainty estimates. In early stages of training or in noisy environments, these estimates can be unreliable, leading to poor weighting decisions and suboptimal learning trajectories. Third, in tasks with well-shaped and high-quality reward functions, the presence of an SFT loss may actually slow down convergence to the optimal policy, as it introduces additional constraints. Fourth, the simultaneous presence of two learning objectives complicates debugging and interpretability; it becomes harder to pinpoint the root cause of training failures. Fifth, when SFT data is low-quality or misaligned with reward criteria, retaining its influence throughout training may degrade performance. Finally, from a practical standpoint, jointly maintaining both loss signals increases computational cost and training complexity—particularly in large-scale or multi-model setups.

Given these trade-offs, we recommend using soft fusion methods like SuperRL in domains that demand generalization, stability, and human-alignment under weak or partially specified reward functions. Such domains include open-domain question answering, value-sensitive decision making, and instruction tuning with sparse preference feedback. In contrast, SFT+RL may remain a preferable alternative in settings with dense, trustworthy rewards and high alignment between demonstrations and task incentives, such as games, synthetic environments, or simulation-based agents.

In summary, SuperRL offers a principled alternative to hard switching by integrating imitation and exploration in a unified and adaptive manner. Although it introduces additional complexity, its benefits in generalization, sample efficiency, and robustness make it a compelling choice for real-world LLM training scenarios that demand flexibility and long-horizon reasoning.